

# Global deletion of MGL in mice delays lipid absorption and alters energy homeostasis and diet-induced obesity

John D. Douglass,<sup>1,\*</sup> Yin Xiu Zhou,<sup>\*</sup> Amy Wu,<sup>\*</sup> John A. Zadrogra,<sup>\*</sup> Angela M. Gajda,<sup>\*</sup> Atreju I. Lackey,<sup>\*</sup> Wensheng Lang,<sup>†</sup> Kristen M. Chevalier,<sup>†</sup> Steven W. Sutton,<sup>†</sup> Sui-Po Zhang,<sup>†</sup> Christopher M. Flores,<sup>†</sup> Margery A. Connelly,<sup>2,†</sup> and Judith Storch<sup>3,\*§</sup>

Department of Nutritional Sciences\* and Rutgers Center for Lipid Research, School of Environmental and Biological Sciences,<sup>§</sup> Rutgers University, New Brunswick, NJ 08901; and Janssen Research & Development, LLC,<sup>†</sup> Spring House, PA 19477

**Abstract** Monoacylglycerol lipase (MGL) is a ubiquitously expressed enzyme that catalyzes the hydrolysis of monoacylglycerols (MGs) to yield FFAs and glycerol. MGL contributes to energy homeostasis through the mobilization of fat stores and also via the degradation of the endocannabinoid 2-arachidonoyl glycerol. To further examine the role of MG metabolism in energy homeostasis, MGL<sup>-/-</sup> mice were fed either a 10% (kilocalories) low-fat diet (LFD) or a 45% (kilocalories) high-fat diet (HFD) for 12 weeks. Profound increases of MG species in the MGL<sup>-/-</sup> mice compared with WT control mice were found. Weight gain over the 12 weeks was blunted in both diet groups. MGL<sup>-/-</sup> mice were leaner than WT mice at both baseline and after 12 weeks of LFD feeding. Circulating lipids were decreased in HFD-fed MGL<sup>-/-</sup> mice, as were the levels of several plasma peptides involved in glucose homeostasis and energy balance. Interestingly, MGL<sup>-/-</sup> mice had markedly reduced intestinal TG secretion following an oral fat challenge, suggesting delayed lipid absorption. Overall, the results indicate that global MGL deletion leads to systemic changes that produce a leaner phenotype and an improved serum metabolic profile.—Douglass, J. D., Y. X. Zhou, A. Wu, J. A. Zadrogra, A. M. Gajda, A. I. Lackey, W. Lang, K. M. Chevalier, S. W. Sutton, S-P. Zhang, C. M. Flores, M. A. Connelly, and J. Storch. **Global deletion of MGL in mice delays lipid absorption and alters energy homeostasis and diet-induced obesity.** *J. Lipid Res.* 2015. 56: 1153–1171.

**Supplementary key words** monoacylglycerols • monoglycerides • monoacylglycerol lipase

Monoacylglycerols (MGs) are intermediates within a large network of lipid molecules used for energy production,

*These studies were supported in part by US National Institutes of Health Grant DK38389 (J.S.), the New Jersey Agricultural Experiment Station, and Janssen Research & Development, LLC. W.L., K.M.C., S.W.S., S-P.Z., C.M.F., and M.A.C. are currently or have been employed by Janssen Research & Development, LLC.*

*Manuscript received 13 February 2015.*

*Published, JLR Papers in Press, April 4, 2015  
DOI 10.1194/jlr.M058586*

Copyright © 2015 by the American Society for Biochemistry and Molecular Biology, Inc.

This article is available online at <http://www.jlr.org>

energy storage, membrane components, and signaling. Extracellular hydrolysis of dietary TG in circulating lipoproteins yields FFAs and *sn*-2 MG, which are then taken up by cells (1, 2). MGs are also produced intracellularly from membrane phospholipids and the consecutive action of phospholipase C and diacylglycerol lipase, or from the hydrolysis of stored TG by adipose TG lipase (ATGL) and hormone sensitive lipase (HSL) (2–5). The ultimate fate of intracellular MGs is hydrolysis to FFAs and glycerol or reesterification by acyltransferases into diacylglycerol and TG (6, 7).

MG lipase (MGL) is considered the rate-determining enzyme in MG catabolism. MGL accounts for roughly 85% of MG hydrolysis in the brain, with the remainder being catalyzed by the enzymes ABHD6 and ABHD12 (8, 9). MGL is expressed in many other tissues as well, including brain, liver, skeletal muscle, adipose, and intestine (10–13). Within cells, MGL localizes to both the cytosolic and membrane fractions and hydrolyzes *sn*-1 and *sn*-2 MGs of varying acyl chain lengths and degrees of unsaturation, with almost no activity toward other lipids, such as TG and lyso-phospholipids (10, 14–18).

MGL is involved in energy balance through two important functions. First, in its well-established role of mobilizing

Abbreviations: AA, arachidonic acid; AEA, arachidonoyl ethanolamide; 2-AG, 2-arachidonoyl glycerol; AUC, area under the curve; CB, cannabinoid; EC, endocannabinoid; HFD, high-fat diet; HOMA-IR, homeostatic model assessment of insulin resistance; iMGL, mice that over-express monoacylglycerol lipase specifically in the intestinal mucosa; LFD, low-fat diet; MG, monoacylglycerol; MGL, monoacylglycerol lipase; OFTT, oral fat tolerance test; OGTT, oral glucose tolerance test; RER, respiratory exchange ratio.

<sup>1</sup> Present address of J. D. Douglass: Division of Metabolism, Endocrinology, and Nutrition, Department of Medicine, University of Washington, Seattle, WA 98109.

<sup>2</sup> Present address of M. A. Connelly: LipoScience, 2500 Sumner Blvd, Raleigh, NC 27616.

<sup>3</sup> To whom correspondence should be addressed.  
e-mail: [storch@aesop.rutgers.edu](mailto:storch@aesop.rutgers.edu)

cellular lipid stores in adipose and other tissues, MGL makes glycerol and FFAs available for a variety of purposes, including  $\beta$ -oxidation. Second, MGL has been recently shown to be a key regulator of levels of the endocannabinoid (EC), 2-arachidonoyl glycerol (2-AG) (19). 2-AG, along with arachidonoyl ethanolamide (AEA) (also known as anandamide), are the two most prominent endogenous ligands of the cannabinoid (CB) receptors CB1 and CB2 (20). While the EC system is involved in the regulation of many physiological systems throughout the body, the net metabolic effect of CB1 activation, acutely, is energy accumulation (20). In the brain, this is mediated by hypothalamic potentiation of orexigenic pathways that stimulate eating behaviors and which are reinforced by the mesolimbic dopamine reward system (21–24). Peripheral CB1 stimulation also enhances fat uptake in adipose tissue, increases de novo lipogenesis in the liver, and decreases energy expenditure in muscle (25–28). Notably, EC activity in the gut also appears to affect eating behaviors, as peripheral administration of CB1 agonists induce acute hyperphagia, an effect potentially mediated by CB1 receptors on vagal afferents that innervate the gastrointestinal tract (29, 30).

Studies of both in vivo pharmacological inhibition and genetic knockout of MGL have focused primarily on its role in the EC system. The potent MGL inhibitor, JZL184, causes 8-fold increases in brain 2-AG levels and cannabimimetic behavioral effects in mice, such as analgesia, hypolocomotion, catalepsy, and hypothermia, the so-called CB tetrad (8, 31). Interestingly, however, in contrast to acute 2-AG elevation, prolonged 2-AG elevation following chronic administration of JZL184 results in desensitization of the central EC system, likely caused by tonic activation of CB1 (32–34). Studies in MGL<sup>-/-</sup> mice recapitulate the effect of chronically elevated 2-AG, demonstrated by CB1 agonist-induced cross-tolerance and a lack of change in core body temperature, locomotion, or nociceptive sensitivity (19, 32). Some metabolic changes have been reported in MGL<sup>-/-</sup> mice, including reduced lipolysis in adipocytes and improved insulin sensitivity after 12 weeks of very high-fat feeding (35). However, MGL<sup>-/-</sup> mice have not been found to have increased body weight gain relative to WT mice, as might be expected from elevated 2-AG levels. In fact, one study of MGL<sup>-/-</sup> mice showed a reduction in body weight, whereas another showed no change, relative to WT mice (19, 35).

In previous studies, we identified MGL transcript and protein expression in rat and mouse small intestinal mucosa; and subsequent studies in mice revealed that normally low levels of MGL expression and activity in adult mucosa could be increased through high-fat feeding, suggesting nutritional regulation and a possible role for MGL in dietary lipid assimilation (36, 37). To further explore this potential role of intestinal MGL, we generated a transgenic mouse that overexpressed MGL specifically in the intestinal mucosa (iMGL mice) (13). LC/MS analyses showed decreased mucosal levels of MG, notably 2-AG, as well as decreased levels of AEA. While the iMGL mice showed normal intestinal FA and MG metabolism, they developed a remarkably obese phenotype after only 3 weeks of 40% kcal HFD feeding,

which was secondary to hyperphagia and decreased energy expenditure (13). The increased body weight and fat mass, as well as the hyperphagia, of iMGL mice were perhaps unexpected, given the known orexigenic effects of central CB receptor activation, yet in line with the reported absence of hyperphagia secondary to MGL deletion (35, 38). We suggested, therefore, that gut 2-AG may possibly act as a satiety signal (13).

To further understand the role of MGL in energy homeostasis in the present study, we examined the effects of 12 weeks of semipurified low-fat diet (LFD) and high-fat diet (HFD) feeding in MGL<sup>-/-</sup> mice. Overall, the results demonstrate systemic changes that led to a leaner phenotype in LFD-fed mice and an improved metabolic serum profile in HFD-fed mice. Further, MGL<sup>-/-</sup> mice displayed a marked reduction in the rate of intestinal lipid secretion and a blunting of postprandial lipemia following an oral fat bolus. Therefore, it is possible that inhibiting MGL may be a useful strategy for the treatment of metabolic disorders, including obesity and its comorbidities.

## MATERIALS AND METHODS

### Generation of MGL knockout mice

The MGL<sup>-/-</sup> mouse strain was purchased from Lexicon Genetics, Inc. (Woodlands, TX) and the colony was bred and housed at Ace Animals (SAGE Labs, Boyertown, PA). Briefly, MGL<sup>-/-</sup> mice were generated from an OmniBank ES cell clone, OST113734 (39), containing a gene trap cassette insertion in the second intron of MGL (accession number NM\_011844). Mice were originally derived on a 129/SvEv background and were backcrossed to C57BL/6 for 10 generations. Quantitative TaqMan RT-PCR was performed to detect mouse MGL mRNA in RNA samples extracted from MGL<sup>+/+</sup>, MGL<sup>+/-</sup>, and MGL<sup>-/-</sup> mice. Multiple mouse tissues were isolated, and mRNA was extracted using RNAqueous Micro kit (Ambion). cDNA reverse transcription was performed on the isolated mRNA, using a high-capacity cDNA reverse transcription kit (Applied Biosystems, Foster City, CA). Purified cDNA was quantified with Quant-iT OliGreen ssDNA reagent (Invitrogen) to ensure equal loading of cDNA in each reaction. TaqMan gene expression oligonucleotides for MGL (Mm00449275\_m1; made to order) were purchased from Applied Biosystems. Quantitative PCR reactions were performed with an ABI Prism 7000 sequence detection system (Applied Biosystems).

### MGL activity assay

MGL<sup>+/+</sup>, MGL<sup>+/-</sup>, and MGL<sup>-/-</sup> mouse brains were isolated from Lexicon mice. One gram of mouse brain was homogenized in 10 ml of MGL buffer (20 mM piperazine-N,N'-bis(2-ethanesulfonic acid), 150 mM NaCl, and 0.001% Tween at pH 7.0) using a Polytron pestle homogenizer (speed 10.2, three times for 15 s) on ice. Protein concentrations were determined using the Bradford assay (BioRad Laboratories, Hercules, CA), and samples were adjusted to 1 mg/ml. To a polypropylene block (1,000  $\mu$ l size), final concentrations of 1.65  $\mu$ g/well brain homogenate, 4 nM [<sup>3</sup>H]2-AG (American Radiolabeled Chemicals, St. Louis, MO), and 10  $\mu$ M cold 2-AG (Sigma-Aldrich, St. Louis, MO) were added (final volume 250  $\mu$ l). The contents were shaken at 37°C for 90 s at 750 rpm, and then incubated for 10 min at 37°C. In a separate tube, activated acid-washed charcoal was prepared to 25 mg/ml in TE buffer, pH 7.4 (10 mM Tris, 1 mM EDTA). This solution was further diluted to 8.125 mg/ml

in 0.5 M HCl. To each well of the polypropylene block, 400  $\mu$ l of activated acid-washed charcoal (Sigma-Aldrich) was added to a final concentration of 5 mg/ml. The contents were shaken at 37°C for 90 s at 750 rpm, incubated at room temperature for 30 min, and then centrifuged at 2,000 *g* for 10 min at room temperature. The supernatants (40  $\mu$ l) were carefully removed without disturbing the charcoal and combined with Scint 20 fluid (160  $\mu$ l) (Perkin Elmer, Waltham, MA) into an Opti-96-well plate (Perkin Elmer), which was shaken for 1 min at 750 rpm and incubated for 1 h at room temperature. The plate was then read on a Top Count (Perkin Elmer) to measure the amount of [<sup>3</sup>H]glycerol in the supernatant cocktail (cpm). The cpm were converted to millimoles per minute per milligram protein according to the following equation: protein (mmol/min/mg) = cpm  $\times$  (dpm 100%/cpm 30%)  $\times$  [1 uCi/(2.2  $\times$  10<sup>6</sup> dpm)]  $\times$  mmol/16 uCi  $\times$  1/10 min  $\times$  1/0.0016 mg.

### Feeding study, surgical procedures, and tissue collection

Age-matched 7-week-old WT mice and MGL<sup>-/-</sup> mice were imported to the Rutgers University animal facility from Ace Animals (SAGE Labs). Several pairs of heterozygous breeding mice were also imported to generate mice for the real-time food intake, oral fat tolerance tests (OFTTs), and radiolabeled intestinal lipid metabolism experiments. The same feeding study protocol was repeated for both male and female groups. All mice were fed Purina 5015 rodent chow (60% carbohydrate, 12% fat, and 28% protein by kilocalories) for a week before the start of the study. The animal facility was temperature controlled with a daily 12 h light/dark cycle and ad libitum access to food and water. At 8 weeks of age, the mice were randomized to dietary group according to body weight and housed in individual cages. For the 12 week feeding period, one-half of the mice in each genotype was fed either a 10% kcal LFD (D12450B; Research Diets Inc., New Brunswick, NJ) or a 45% kcal HFD (D12451; Research Diets Inc.) (Table 1). Twice weekly food and body weight measurements were taken. Rodent diets were refreshed weekly and food intake was measured by pellet weight and then converted to total calories consumed. For necropsy, mice were fasted for 12 h prior and injected intraperitoneally with a ketamine-xylazine-acepromazine

cocktail (54.5:45:0.8 mg/kg, respectively) to induce deep anesthesia, followed by exsanguination by the aortic artery for collection of blood. Whole blood samples in EDTA-coated tubes were immediately centrifuged, and the plasma was collected and stored at -70°C. The small intestine from pylorus to cecum was excised and rinsed twice with saline, and the mucosal cells were collected by scraping with a glass slide. Liver, brain, and adipose depots (gonadal, inguinal, retroperitoneal, and intrascapular brown fat) were also collected. All tissues were weighed, snap-frozen on dry ice-ethanol, and stored at -70°C. All animal procedures were approved by the Rutgers University Animal Use Protocol Review Committee and conformed to the National Institutes of Health *Guide for the Care and Use of Laboratory Animals*.

### Body composition, activity, and indirect calorimetry

During the first week and at week 10 of the feeding study, fat mass and lean body mass were analyzed in nonanesthetized mice by MRI, using an EchoMRI-100 (Echo Medical Systems, Houston TX). After the 10 week MRI measurement, mice were immediately acclimatized to individual OxyMax metabolic cages (Columbus Instruments, Columbus, OH) for 24 h prior to 24 h of data collection, during which they were given ad libitum access to water and their respective diets. Respiratory exchange ratio (RER) as VCO<sub>2</sub>/VO<sub>2</sub> was used to determine substrate utilization, and energy expenditure was calculated using: energy expenditure (kcal/kg/h) = (3.815 + 1.232  $\times$  RER) (VO<sub>2</sub>)/(kilograms fat free mass) (40). Locomotor and rearing activities were measured as the number of horizontal or vertical infrared beam breaks, respectively, over a 24 h period.

### Tissue lipid extraction and analyses

Brain, liver, gonadal fat, and mucosa samples were homogenized with 1 $\times$  PBS (pH 7.4) on ice with a Dounce homogenizer and a Wheaton overhead stirrer at 5,000 rpm. Total tissue protein concentration was determined by the Bradford assay (41) and used to standardize the volume of homogenate to extract lipid, as described previously (42). The appropriate amounts of mononanoin (C9:0) and 10Z-heptadecenoyl (C17:1) ethanolamide were added as internal standards to each sample of brain (12 mg protein), liver (10 mg), intestinal mucosa (10 mg), and

TABLE 1. Diet composition

Diet	LFD: D1450B		HFD: D12451	
	Grams (%)	Kilocalories (%)	Grams (%)	Kilocalories (%)
Protein	19.2	20	24	20
Carbohydrate	67.3	70	41	35
Fat	4.3	10	24	45
Total		100		100
Kilocalories per gram	3.85		4.73	
Ingredient				
Casein, 80 mesh	200	800	200	800
L-cystine	3	12	3	12
Corn starch	315	1,260	72.8	291
Maltodextrin 10	35	140	100	400
Sucrose	350	1,400	172.8	691
Cellulose, BW200	50	0	50	0
Soybean oil	25	225	25	225
Lard	20	180	177.5	1,598
Mineral mix S10026	10	0	10	0
Dicalcium phosphate	13	0	13	0
Calcium carbonate	5.5	0	5.5	0
Potassium citrate, 1 water	16.5	0	16.5	0
Vitamin mix V10001	10	40	10	40
Choline bitartrate	2	0	2	0
FD and C yellow dye #5	0.05	0	0	0
FD and C red dye #40	0	0	0.05	0
Total	1,055.05	4,057	858.15	4,057

gonadal fat (1 mg) homogenate. Lipid extractions were then performed using the Folch procedure (43), and samples were dried down under nitrogen gas and reconstituted in chloroform.

Tissue MG and acylethanolamide levels were determined by LC/MS. To be compatible with the reverse-phase LC system, an aliquot of 100  $\mu$ l of each lipid extract in chloroform was transferred into a 350  $\mu$ l glass insert on a 96-well plate. Solvent was removed under nitrogen gas, and the residue was reconstituted with 100  $\mu$ l of tetrahydrofuran-isopropyl alcohol (20:80). The final solution (10  $\mu$ l) was injected onto an Agilent 1100 series LC/MS/MS system (Agilent Technologies, Palo Alto, CA) and a Waters Quattro Premier triple quadrupole mass spectrometer (Waters, Milford, MA). Separation of the analytes was performed on a Zorbax Eclipse XDB-C8 column (2.1  $\times$  50 mm) eluted gradually with 50–90% mobile phase B within 5 min, held at 90% B for 3 min, and returned to 30% B in 0.1 min. Mobile phase A was 5 mM ammonium formate and 0.1% formic acid in water and mobile phase B was 5 mM ammonium formate and 0.1% formic acid in acetonitrile-water (95:5). The flow rate was set at 0.3 ml/min. The mass spectrometer was operated in the positive ion mode, and multiple reaction monitoring was used for quantification. The mass transitions for detection of acylethanolamides were protonated molecular ion > protonated ethanolamine (*m/z* 62.0) at a collision energy of 15 eV. The mass transitions for MG were protonated molecular ion > acylidynonium at a collision energy of 20 eV. Quantification of each analyte was achieved based on the relative peak area ratio of the analyte to the internal standard calibrated with the corresponding response factor. MassLynx software version 4.0 was used for system control and data processing.

### Real-time food intake measurements

Real-time monitoring of food intake was measured using BioDAQ instrumentation (Research Diets, Inc.) (44). After 12 weeks of 10% LFD feeding, WT and MGL<sup>-/-</sup> mice were acclimated to BioDAQ cages for 5 days, followed by 7 days of continuous data collection. Food pellets were the same as during the feeding study and were refreshed daily for each cage to ensure no loss from spillage. Individual feeding bouts were determined by changes in food hopper weight greater than 0.02 g. Meals were

defined as the sum total of feeding bouts that occurred within a 5 min period of each other.

### OFTT and fat absorption localization study

After 12 weeks of 10% LFD or 45% HFD feeding, mice were fasted for 16 h prior to the OFTT. At time = 0 (*t*<sub>0</sub>), the mice were given a 500 mg/kg body weight ip injection of tyloxapol (Triton WR-1339) to block peripheral lipoprotein clearance. Thirty minutes following tyloxapol injection, 300  $\mu$ l of olive oil was given by orogastric gavage. Blood samples were collected from the tail at time = 0 (*t*<sub>0</sub>), 60, 120, 180, and 240 min, and TG levels were assessed in 15  $\mu$ l of whole blood by Cardiochek lipid analyzer (Polymer Technology Systems Inc., Zionsville, IN).

Fat absorption localization experiments were performed to analyze the anatomical distribution of lipid absorption along the length of the small intestine. Mice were fed a 10% LFD for a period of 12 weeks. Following a 4.5 h fast, mice were gavaged with 8  $\mu$ Ci of <sup>3</sup>H-labeled TG in 200  $\mu$ l olive oil. The mice were then anesthetized 1.5 h after the gavage and the small intestine was excised, rinsed with 0.85% NaCl, and then cut into 2 cm sections. The intestinal sections were digested overnight in 500  $\mu$ l of 1 M NaOH at 60°C. The next day 300  $\mu$ l of 1 N HCl was added to quench, and the radioactivity of each section was measured in a scintillation counter.

### RNA extraction and real-time PCR analysis

Total mRNA was extracted from tissues following the 12 week feeding study using a modified method from Chomczynski and Sacchi (45) and analyzed as previously described (46). In brief, frozen tissues were homogenized in 4 M guanidinium thiocyanate with an Ultra-Turrax IKA-Werke (Wilmington, DE). Total RNA was isolated by phenol extraction, followed by precipitation and washing with ethanol. The RNA was further purified by removal of genomic DNA by DNase digest and RNeasy cleanup kit (Qiagen, Valencia, CA). The integrity of the RNA was assessed by gel electrophoresis and visualization of the 18S and 23S rRNA subunits. Reverse transcription was performed on 2  $\mu$ g of RNA using a high-capacity cDNA kit (Promega, Madison, WI). Primer sequences shown in **Table 2** were obtained from

TABLE 2. Primer sequences used for RT-PCR analyses

Gene	Function	Primer	Sequence
$\beta$ -actin	Housekeeping	Forward	5'-GGCTGTATTCCTCCATCG-3'
		Reverse	5'-CCAGTTGGTAACAATGCCATGT-3'
MGAT2	TG synthesis	Forward	5'-TGGGAGCGCAGGTACAGA-3'
		Reverse	5'-CAGGATGGCATAACAGGACAGA-3'
GPAT3	TG synthesis	Forward	5'-TATCCAAAGAGATGAGTCACCCA-3'
		Reverse	5'-CACAATGGCTTCCAACCCCTT-3'
GPAT1	TG synthesis	Forward	5'-CTGCTTGCCTACCTGAAGACC-3'
		Reverse	5'-GATACGGCGGTATAGGTGCTT-3'
DGAT1	TG synthesis	Forward	5'-TCCGTCCAGGGTGGTAGTG-3'
		Reverse	5'-TGAACAAAGAATCTTGCAGACGA-3'
DGAT2	TG synthesis	Forward	5'-TTCCTGGCATAAGGCCCTATT-3'
		Reverse	5'-AGTCTATGGTGTCTCGGTTGAC-3'
MGL	MG hydrolysis	Forward	5'-CAGAGAGGCCACCTACTTTT-3'
		Reverse	5'-ATGCGCCCAAGGTCATATT-3'
ACCL1	Lipogenesis	Forward	5'-AGGTGGTGATAGCCGGTATGT-3'
		Reverse	5'-TGGGTAATCCATAGAGCCAG-3'
FAS	Lipogenesis	Forward	5'-ATGGGCGGAATGGTCTCTTTC-3'
		Reverse	5'-TGGGGACCTTGTCTTCATCAT-3'
FAAH	Acylethanolamide hydrolysis	Forward	5'-GAGGCTCCCCTCTGGGTTTA-3'
		Reverse	5'-GCCAGGCTATCCACATCCC-3'
CB1	CB receptor	Forward	5'-GGGCACCTTCACGGTTCTG-3'
		Reverse	5'-GTGGAAGTCAACAAAGCTGTAGA-3'
NPY	Orexigenic neuropeptide	Forward	5'-ATGTAGGTAACAAGCGAATGG-3'
		Reverse	5'-TGTCCGAGAGCGGAGTAGTAT-3'
AgRP	Orexigenic neuropeptide	Forward	5'-ATGCTGACTGCAATGTTGCTG-3'
		Reverse	5'-CAGACTTAGACCTGGGAACCTCT-3'

Sigma-Aldrich. The efficiency ( $100 \pm 5\%$ ) of each PCR primer set was first assessed by standard curve. Real-time PCR was performed in triplicate using the ddCT method on an ABI 7300 PCR instrument (Applied Biosystems). Each reaction contained 80 ng of cDNA, 250 nM of each forward and reverse primer, and 12.5  $\mu$ l of POWER SYBR Green Master Mix (Applied Biosystems) in a total volume of 25  $\mu$ l.  $\beta$ -Actin was used as the endogenous control for each standard, and the relative quantitation of each gene was determined with respect to the average of the WT LFD-fed mice.

### Plasma analyses

Plasma samples were obtained during the necropsy as described above. TG, cholesterol, NEFA, and adiponectin levels were measured by colorimetric assay (WAKO Diagnostics, Richmond, VA). All other plasma peptide analytes were determined by immunoassay using a MAGPIX instrument (Luminex Corp., Austin, TX) and a Milliplex multiplex panel for mouse metabolic hormones (Millipore, Billerica, MA).

### Glucose tolerance test and insulin resistance

After 11 weeks of LFD or HFD feeding, the mice were fasted for 6 h prior to the oral glucose tolerance test (OGTT) and then given a bolus of 2 g/kg body weight D-(+)-glucose solution by oral gavage. Blood glucose was measured using a glucometer at time = 0, 30, 60, and 120 min after collecting blood from tail nicks (Accucheck, Roche Diagnostics). Homeostatic model assessment of insulin resistance (HOMA-IR) (47) was calculated using  $\text{HOMA-IR} = \text{fasted glucose (mg/dl)} \times \text{fasted insulin (mU/l)} / 405$ .

### Statistical analyses

A total of 50 mice (six to seven females per group and six males per group) were used in this study. Females and males were compared both independently and together using the WT LFD group averages to normalize data for each sex. All group data are shown as average  $\pm$  SEM. Statistical comparisons were determined between genotypes on the same diet using a two-sided Student's *t*-test. One-way ANOVA with Tukey's post hoc comparison, repeat measures ANOVA, and linear regression were performed using JMP 10 statistical software (SAS Institute Inc.). Differences were considered significant for  $P < 0.05$ . Area under the curve (AUC) for the OGTT was calculated using the trapezoid rule.

## RESULTS

### Genetic knockout of MGL in mice

While mice generated from this Lexicon MGL deletion construct have been utilized in previous studies (32, 48), we first assessed the absence of MGL gene expression in our MGL-null strain to confirm its resultant loss of function. MGL mRNA was absent in all tissues collected from the knockout mice. Brain transcript levels of MGL were significantly reduced in heterozygous  $\text{MGL}^{+/-}$  mice and undetectable in  $\text{MGL}^{-/-}$  mice (Fig. 1A). The activity of MGL was determined in whole brain homogenates and demonstrated that catabolism of 2-AG was reduced by 30% in  $\text{MGL}^{+/-}$  mice and by 83% in  $\text{MGL}^{-/-}$  mice compared with WT counterparts (Fig. 1B). These results confirm the absence of MGL expression and its effect on MG hydrolytic activity in the brain.

### Tissue MG and acylethanolamide levels in $\text{MGL}^{-/-}$ mice

The effects of MGL genetic deletion on MG and acylethanolamide species in various tissues were examined by LC/MS. For these and all subsequent analyses, results were generally similar for male and female test groups. Thus, there were profound increases of MG species in the brain, liver, and epididymal fat of both LFD- and HFD-fed  $\text{MGL}^{-/-}$  mice (Fig. 2A–C). Notably, whole brain 2-AG levels were increased 92- to 131-fold in  $\text{MGL}^{-/-}$  mice compared with WT levels (Fig. 2A). In contrast to those observed in brain, liver, and adipose tissue, there were only modest elevations in several MG species in intestinal mucosa (Fig. 2D). Acylethanolamide levels, including AEA, were not substantially altered in adipose tissue or intestinal mucosa (Fig. 3C, D). However, some brain and liver acylethanolamides were increased, particularly in the HFD-fed  $\text{MGL}^{-/-}$  mice (Fig. 3A, B).

### Alterations in body mass and composition with MGL deletion

There were no differences in body weight for either group of mice at the beginning of the experiment. Over 12 weeks of feeding, however, lower body weights in both

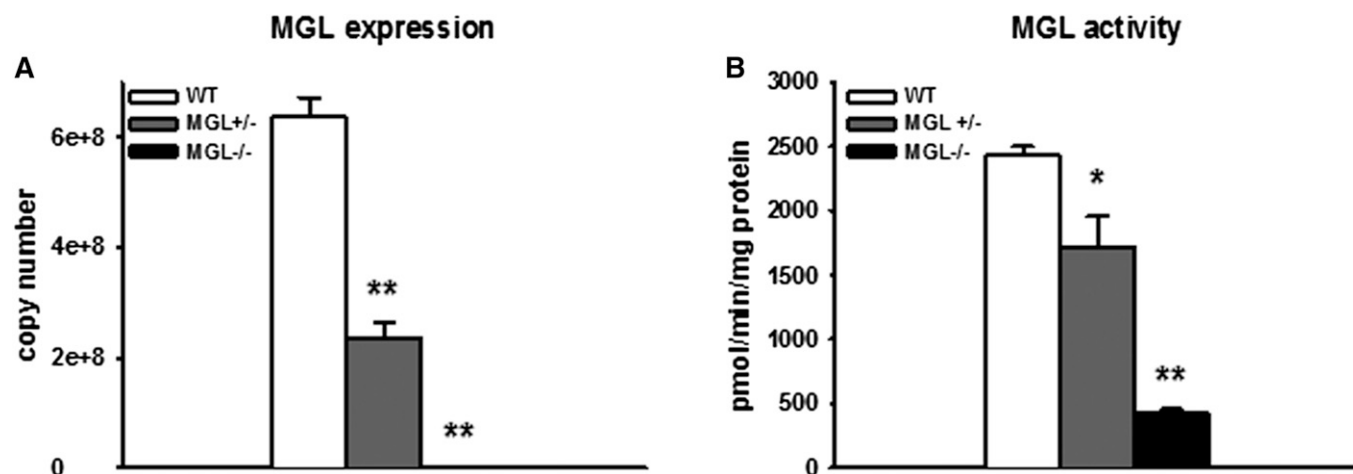


Fig. 1. Absence of MGL expression and function in  $\text{MGL}^{-/-}$  mice A: Quantitative PCR of MGL transcript in brain. B: MGL activity determined by [<sup>3</sup>H]2-AG hydrolysis to 2-AG and glycerol in whole brain homogenates. Data are expressed as average  $\pm$  SEM (n = 4–6). \* $P < 0.01$ , \*\* $P < 0.001$  compared  $\text{MGL}^{+/-}$  (WT).

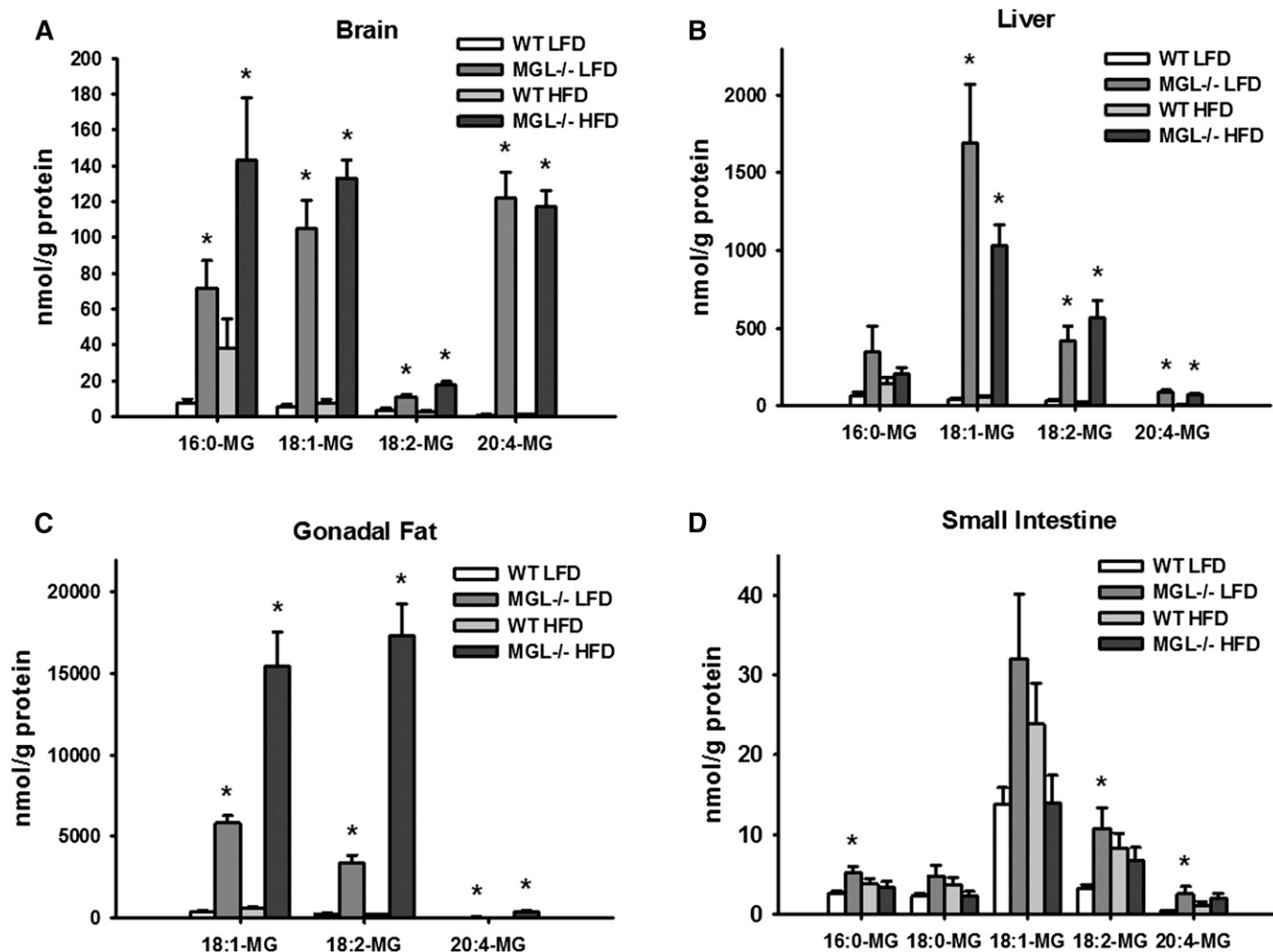


Fig. 2. Tissue content of MG species as determined by LC/MS analysis in brain (A), liver (B), gonadal fat (C), and small intestine mucosa (D). Data are expressed as average  $\pm$  SEM ( $n = 6$ ). \* $P < 0.05$  compared with control group of the same diet.

LFD- and HFD-fed MGL<sup>-/-</sup> mice compared with their WT counterparts were observed (Fig. 4). Using univariate repeated-measures ANOVA, a significant effect of MGL deletion on total body weight for the female LFD-fed group was found (Fig. 4B). Linear regression analyses showed that body weight gain over time was also significantly blunted in the male MGL<sup>-/-</sup> LFD-fed mice ( $P < 0.001$ ), with a similar trend for the HFD-fed mice ( $P = 0.06$ ) (Fig. 4A, B). When results for both males and females on either diet were normalized to WT LFD controls, the effects of the MGL deletion were highly significant ( $P < 0.001$ ). Interestingly, the MGL<sup>-/-</sup> mice were found to be leaner at both baseline and after 12 weeks of LFD feeding, with 33 and 30% less body fat than WT mice, respectively (Fig. 5A). These findings were supported by lower gonadal and retroperitoneal fat pad weights in the same mice (Fig. 5C, D). A trend toward decreased fat mass was also seen in HFD-fed mice, particularly the females; however, the results did not reach statistical significance (Fig. 5A, C, D).

#### Food intake, lipid absorption, and energy utilization in MGL<sup>-/-</sup> mice

During the 12 week dietary intervention, no apparent changes were found in cumulative or average daily food

intake as assessed by pellet weighing (Fig. 6A, B). A separate cohort of male mice was placed into food monitoring cages after being fed the 10% LFD for 12 weeks. Interestingly, using this more sensitive method, it was found that the MGL<sup>-/-</sup> mice consumed more LFD than their WT counterparts during the week of real-time monitoring (Fig. 6C). In particular, the number of meals and the total food intake were increased specifically during the light phase (Fig. 6D, E). No changes in total dietary lipid absorption, as determined by fecal fat content, were observed (Fig. 6F).

Mice were placed in metabolic chambers for indirect calorimetry and activity measurements during the first and last weeks of the 12 week feeding period. Ambulatory activity was monitored by beam breaks over the 24 h collection period. The MGL<sup>-/-</sup> mice displayed a trend toward increased locomotion, however results did not reach statistical significance (Fig. 7A, B, E). During the first week of HFD feeding, the MGL<sup>-/-</sup> mice had lower energy expenditure over the 24 h data collection period (data not shown), but there was no difference between any of the dietary groups at the end of the study (Fig. 7C, D, F). RER values at baseline and after 10 weeks of LFD feeding in MGL<sup>-/-</sup> mice were lower over a 24 h period, indicating

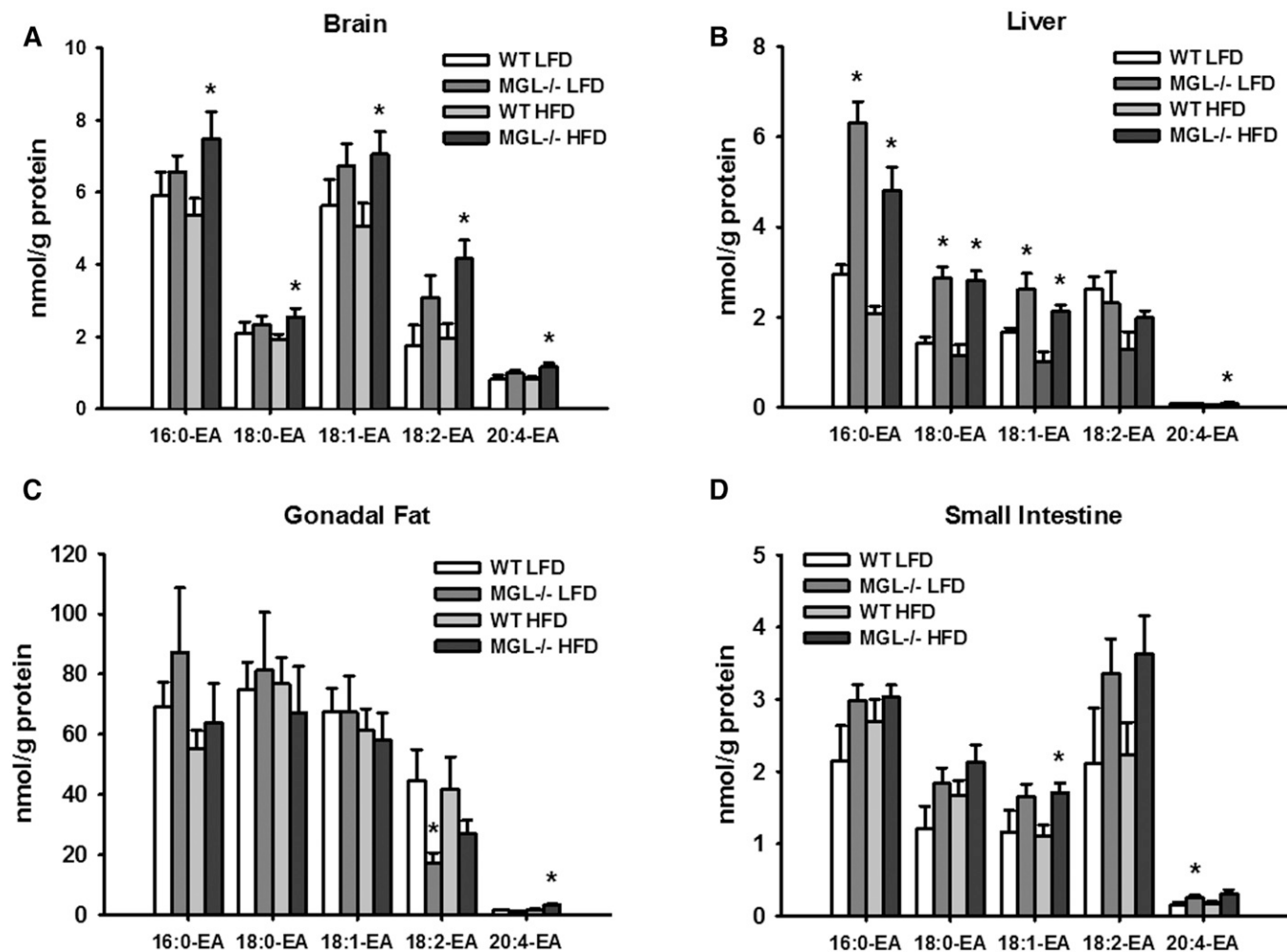


**Fig. 3.** Tissue content of acylethanolamide (EA) species as determined by LC/MS analysis in brain (A), liver (B), gonadal fat (C), and small intestine mucosa (D). Data are expressed as average  $\pm$  SEM ( $n = 6$ ). \* $P < 0.05$  compared with control group of the same diet.

increased fat oxidation, but there were no differences in the HFD-fed mice (Fig. 7G, H).

#### Blunted intestinal TG secretion in MGL<sup>-/-</sup> mice

We assessed intestinal lipid absorption by OFTT in male mice fed the 10 and 45% HFD for 12 weeks. After mice were given an injection with the LPL inhibitor, tyloxapol, and administered an orogastric bolus of olive oil, both groups of MGL<sup>-/-</sup> mice had markedly lower ( $P < 0.01$ ) levels of TG in circulation (Fig. 8A, B). To further investigate whether the localization of intestinal lipid uptake was altered, as has been shown in MGAT2-deficient mice (6), we measured the uptake of an oral fat bolus of <sup>3</sup>H-labeled TG in intestinal sections. No significant differences in the localization of the radiolabeled TG were found in the MGL<sup>-/-</sup> mice, nor was overall uptake affected (Fig. 8C, D).

#### Glycemic control in MGL<sup>-/-</sup> mice

Blockade of EC system signaling via CB1 receptor knockout or chemical inhibition results in improved glucose tolerance in diet-induced obese mice (49, 50). To assess whether glucose disposal is altered in MGL<sup>-/-</sup> mice,

we performed a 2 h OGTT in week 11 of the feeding study. Moderate improvements in glycemic control were observed, with trends for lower blood glucose levels for both LFD- and HFD-fed MGL<sup>-/-</sup> groups (Fig. 9A–C). Lower HOMA-IR values for the HFD-fed MGL<sup>-/-</sup> mice compared with WT further suggest that insulin sensitivity was maintained despite the HFD feeding (Fig. 9D).

#### Circulating lipids and peptides

Reduced serum TG and glycerol levels were found in a previous study of very HFD-fed MGL<sup>-/-</sup> mice (35). In the present study, trends for reduced plasma TG, cholesterol, and NEFA levels were found in both dietary groups of male MGL<sup>-/-</sup> mice. Indeed, when normalized to include both sexes, the HFD-fed MGL<sup>-/-</sup> mice had significantly lower TG, cholesterol, and NEFA levels ( $P < 0.05$  or below, Fig. 10A–C).

Plasma analyses using a multiplex ELISA assay showed a significantly improved metabolic profile of HFD-fed MGL<sup>-/-</sup> mice compared with WT mice. Peptides involved in glucose disposal, such as insulin and C-peptide, were significantly lower, as was the adipocyte-derived hormone, resistin (Table 3).

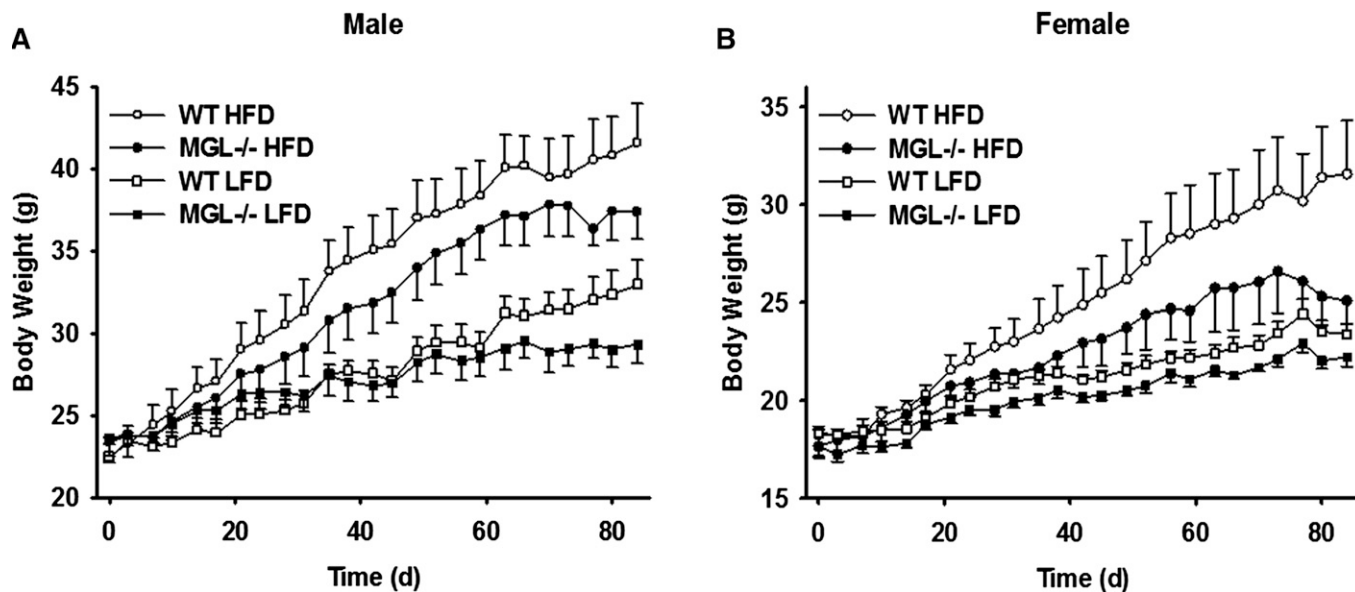


Fig. 4. Body weights during 12 weeks of LFD or HFD feeding in male (A) and female (B) mice. Data are expressed as average  $\pm$  SEM (n = 6).

#### Gene expression in brain, liver, and small intestinal mucosa

The effects of MG deletion and the consequent elevated levels of intracellular MG on the expression of genes encoding for lipid metabolic enzymes and CB receptors were determined. Brain CB1 receptor expression in  $MGL^{-/-}$  mice has been reported to be downregulated (32) or unchanged (19); in the present study, no significant differences in brain CB1 mRNA abundance were observed (Fig. 11A). Expression of the hypothalamic orexigenic peptides, NPY and AgRP, was also unchanged in the brain (Fig. 11A). Additionally, while EC activation has been found to stimulate hepatic de novo lipogenesis via SREBP1c (26), no differences in the expression of its downstream targets, FAS and ACC1, were observed here (Fig. 11A). There were also no changes in hepatic mRNA levels of GPAT1 and GPAT2, proteins which participate in the glycerol-3-phosphate pathway that accounts for the majority of liver and adipocyte TG synthesis (Fig. 11B).

Because the majority of intestinal MG derived from dietary sources is used for TG biosynthesis (51), the expression of lipid metabolic enzymes involved in these processes was measured. Increases in MGAT2, DGAT2, and particularly DGAT1, were observed in both dietary groups of  $MGL^{-/-}$  mice compared with WT mice (Fig. 11C). Conversely, intestinal transcript levels of GPAT1 and GPAT3 were lower in  $MGL^{-/-}$  mice (Fig. 11C).

#### DISCUSSION

The present studies demonstrate that MGL deletion results in lower body weight gain and lower body fat content. The leaner LFD-fed mice also had increased fat oxidation that was not apparent in the HFD-fed mice. This is possibly because reductions in lipolysis have a more pronounced

effect when fat is limited, and is in keeping with the lack of effect in  $MGL$ -null mice fed an extreme 74% kcal HFD (35), as well as the lower body weights reported for animals fed a chow diet (19).  $MGL^{-/-}$  mice fed both LFD and HFD also showed lower levels of serum lipids and an overall trend for lower levels of the circulating metabolic peptides, insulin, C-peptide, leptin, and resistin. It is likely that these reductions are secondary to the decreased fat mass, which is positively correlated with serum lipids and peptides involved in energy homeostasis signaling (52). There was little evidence for either central or peripheral EC activation by the increased tissue levels of 2-AG, consistent with desensitization caused by chronic EC elevation (19, 32, 35).

The reduced body fat and body weight in the  $MGL^{-/-}$  mice does not appear to be secondary to a reduction in food intake or an alteration in energy expenditure, nor have changes in thermogenesis been reported in other studies (19). We did observe a trend toward increased locomotor activity in the  $MGL^{-/-}$  mice, and future studies using longer-term calorimetry may reveal subtle changes in energy expenditure that were not manifested in the present 24 h measurements. It is also worth noting that loss of MG hydrolysis may affect fat stores in other ways. First, desensitization of the EC system may result in functional antagonism, producing effects on fat mass similar to those seen when CB1 is targeted pharmacologically or by genetic deletion (50, 53). This would include the inability to activate CB1 pathways, which would normally inhibit intracellular lipolysis in adipose tissue and FA oxidation in muscle and other tissues (54). Second, the metabolism of excess 2-AG by cyclooxygenase-2 produces prostaglandin glycerol esters (55). It has been proposed that these resultant prostanoids inhibit adipogenesis (56). Thus, an abundance of 2-AG-derived prostaglandin metabolites may be limiting the formation of new adipocytes and thereby causing the diminished fat mass seen in the  $MGL^{-/-}$  mice fed



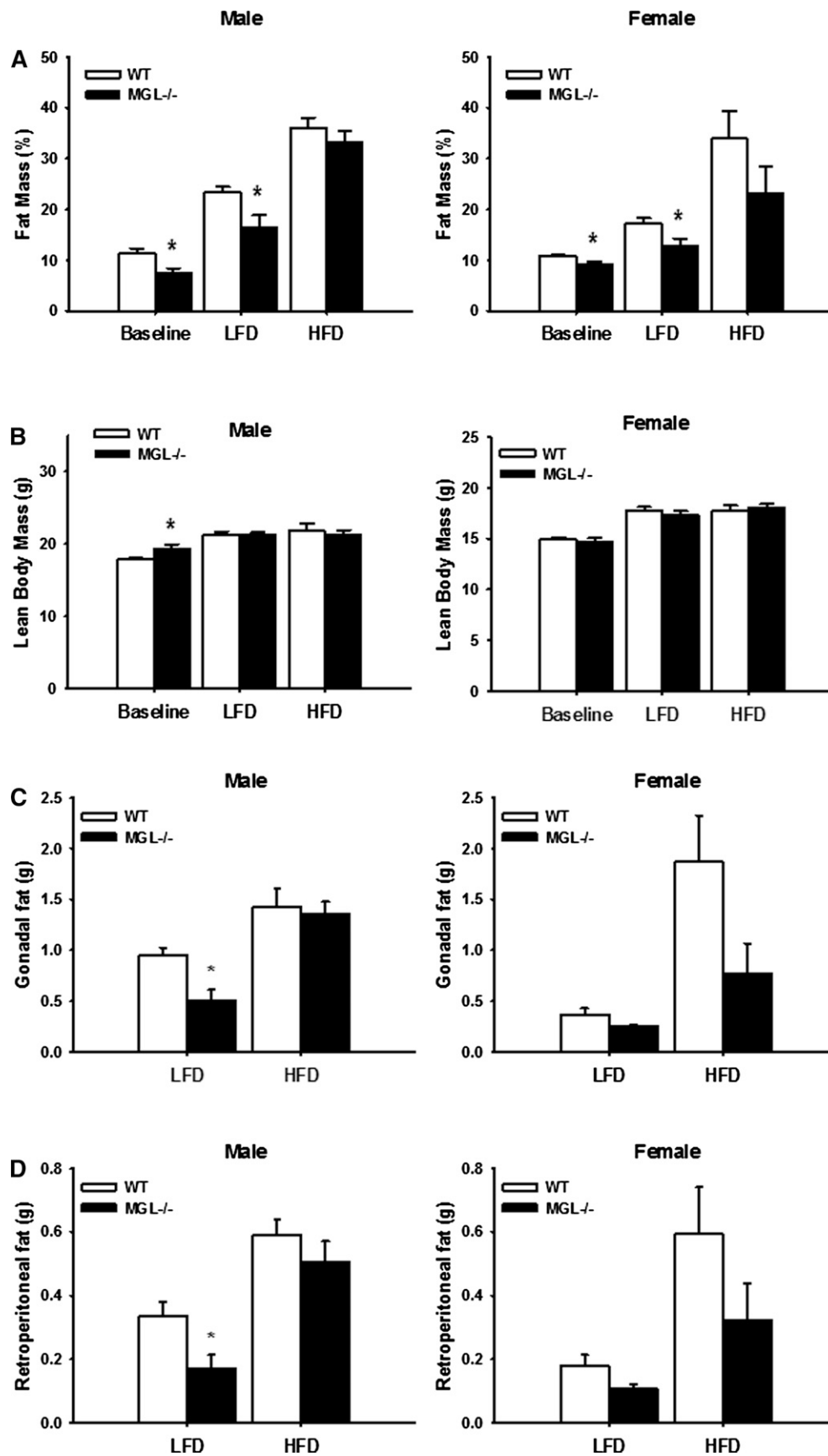
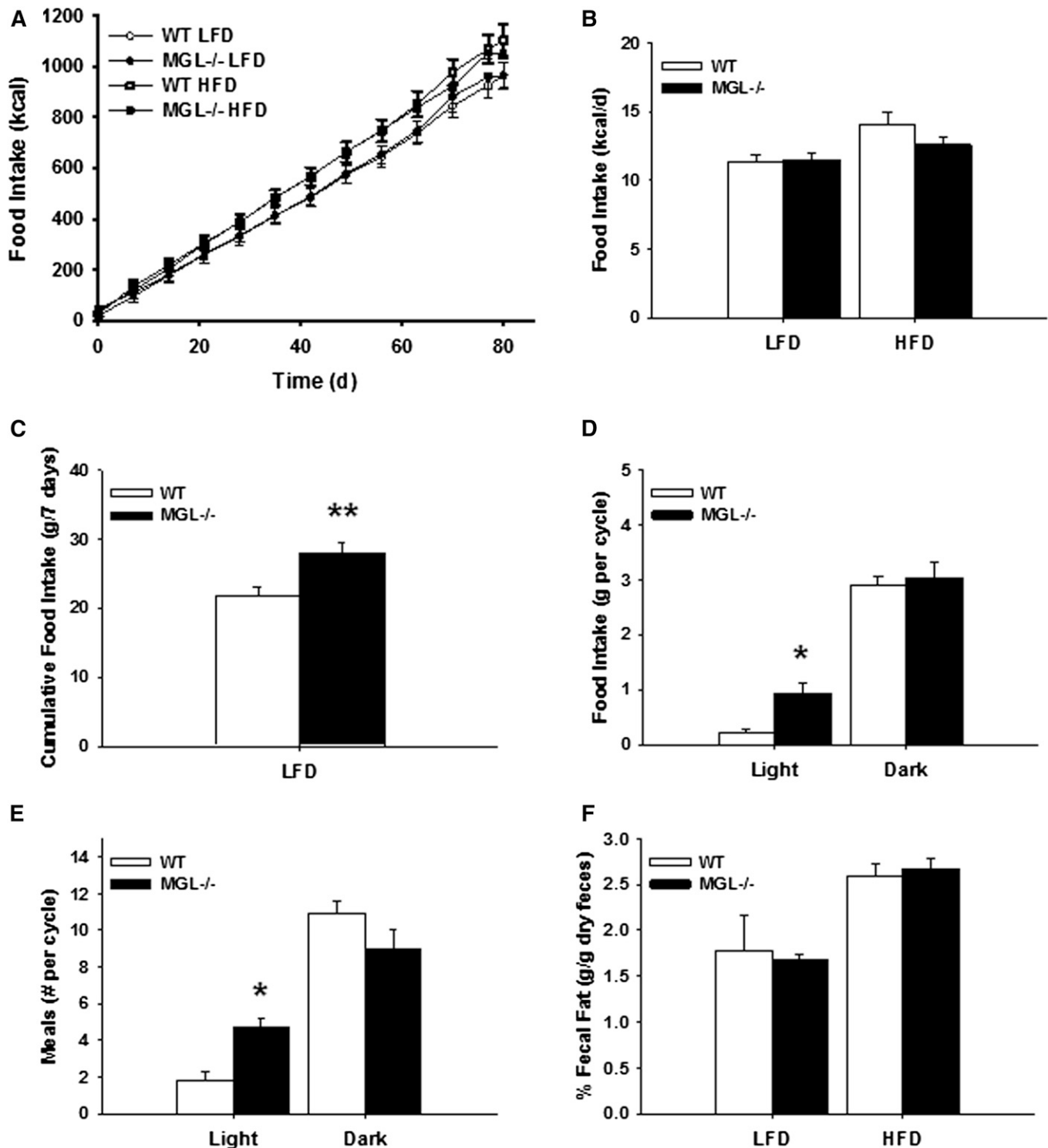


Fig. 5. Body composition and tissue weights in MGL<sup>-/-</sup> mice. A: Fat mass percentage for male and female mice at the beginning (baseline) and after 10 weeks of diet. B: Lean body mass at the beginning (baseline) and end of study. Gonadal (C) and retroperitoneal (perirenal) (D) fat pad weights at necropsy. Data are expressed as average  $\pm$  SEM (n = 6). \* $P < 0.05$  compared with control group of the same diet.



**Fig. 6.** Cumulative and circadian food intake for male mice. Cumulative food intake (A) and average daily food intake (B) during 12 weeks of LFD and HFD feeding. Real time measurement of food intake of LFD after 12 weeks LFD feeding expressed as weekly cumulative food intake (C), food intake per light cycle (D), and number of meals per light cycle (E). F: Fecal fat percentage measured at week 8 of feeding. Data are expressed as average  $\pm$  SEM ( $n = 5-6$ ). \* $P < 0.05$ , \*\* $P < 0.01$  compared with control group of the same diet.

lower fat diets. On the other hand, hypertrophy of existing adipocytes by HFD feeding may mask differences in the fat mass of MGL<sup>-/-</sup> mice, as found here and with very high-fat feeding (35).

The large increases in MG levels in brain, adipose, and liver was expected, based on other studies of MGL<sup>-/-</sup>

mice (19, 32, 35). In brain, the high 2-AG levels are likely reflective of the large 83% reduction in MG hydrolysis that was observed. The remainder of activity may be ascribed to ABHD6 and ABHD12, which had previously been thought to contribute 15% of total brain MG catabolism (9), and is very similar to the residual activity

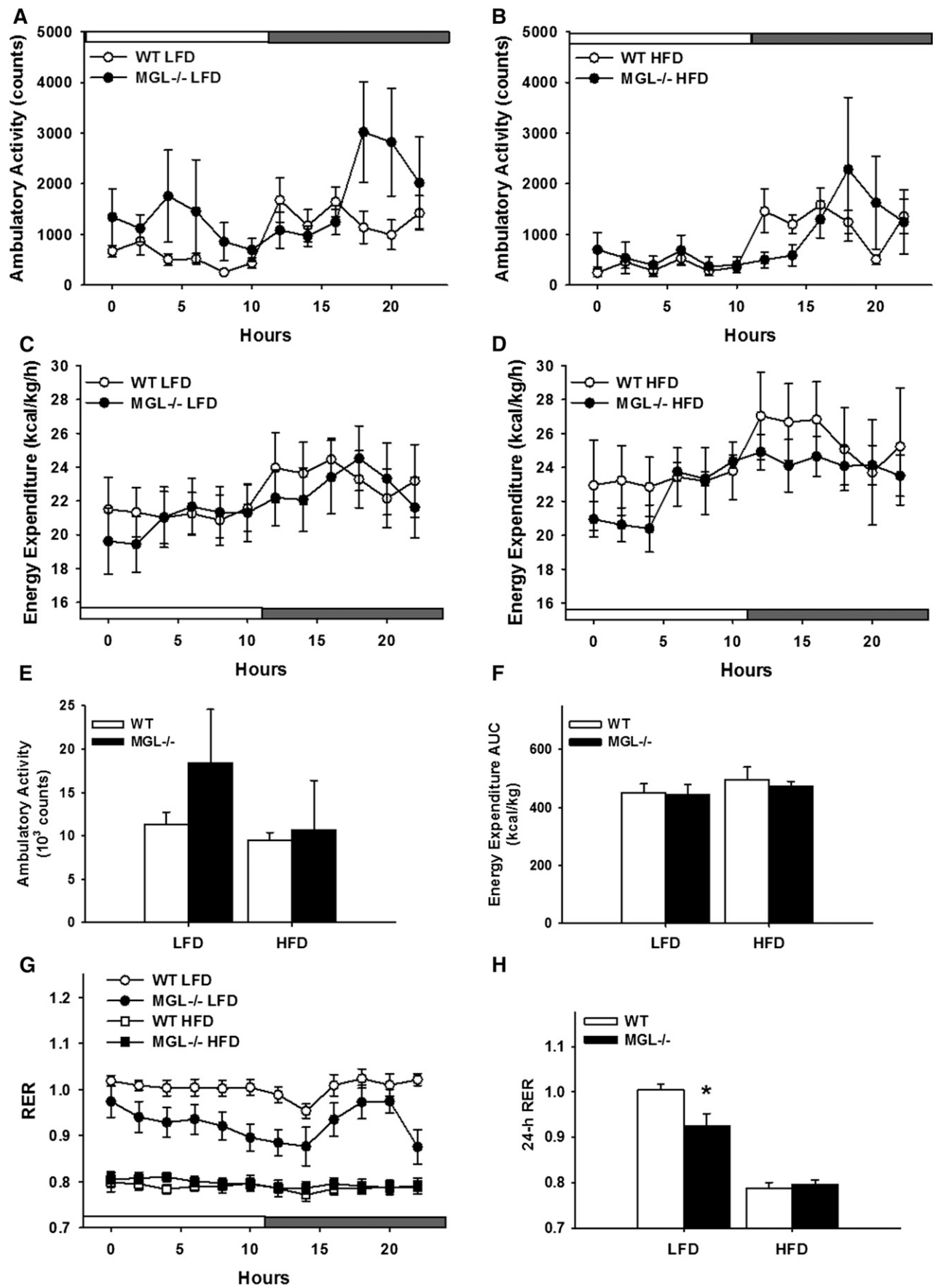


**Fig. 7.** Indirect calorimetry and spontaneous activity for male mice at endpoint (10 weeks of feeding). Ambulatory activity as measured by total consecutive beam breaks for LFD-fed (A) and HFD-fed (B) mice. Energy expenditure expressed per kilogram lean body mass for

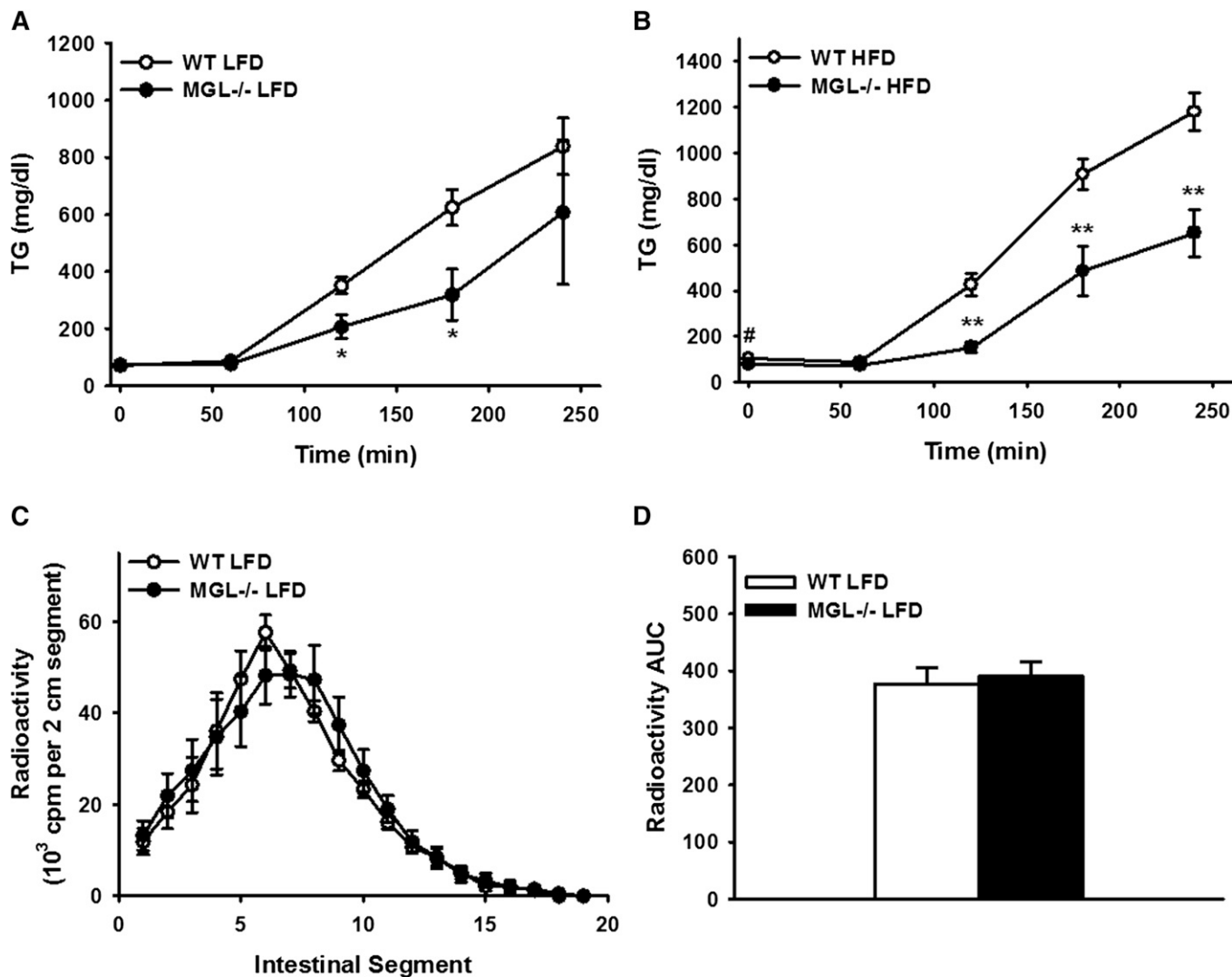


**Fig. 8.** Reduced appearance of TG from an oral fat bolus in the blood of male MGL<sup>-/-</sup> mice. Blood TG levels during OFTT after 12 weeks of LFD (A) and HFD (B) feeding. C: Localization of intestinal lipid absorption 1.5 h after oral gavage with [<sup>3</sup>H]TG and olive oil in mice fed LFD for 12 weeks. D: AUC of total small intestine lipid absorption from localization experiment. Data are expressed as average  $\pm$  SEM (n = 7–8). #*P* = 0.06, \**P* < 0.05, \*\**P* < 0.001 compared with WT.

observed here. It is possible that ABHD6 and ABHD12 may be regulating MG content in certain tissues and cell types. However, mRNA levels of both enzymes were previously found to be unchanged in the brain, liver, and adipose tissue of MGL<sup>-/-</sup> mice (35), indicating a lack of compensatory upregulation. The present results provide further support that MGL is the dominant MG-hydrolyzing enzyme in these major tissues. While other studies of MGL<sup>-/-</sup> mice reported no changes in brain AEA levels (19, 32), modest increases in AEA and other acylethanolamides in liver and brain for both diet groups were observed here. Nevertheless, brain fatty acid amide hydrolase (FAAH) activity in the MGL<sup>-/-</sup> mice was essentially unchanged (data not shown) and therefore cannot account for the increased acylethanolamides.

In the intestinal mucosa, a far more modest effect of MGL deletion on tissue MG levels was observed (Fig. 2D), which may be attributed to a number of factors. First, intestinal MGL expression is low compared with other tissues, such as adipose tissue (13), wherein the lipolytic release of TG pools is a more prominent function. Perhaps more importantly, the resynthesis of TG, using dietary MG and FFA as substrates, is the dominant pathway in the small intestine (51) and serves the vital role of rapidly delivering dietary lipids to the rest of the body. Thus, the 12 h fast prior to necropsy in the animals is likely sufficient time for any excess MG to be reesterified, packaged into chylomicrons, and trafficked into the circulation. Additionally, the observed increase in intestinal MGAT and DGAT enzyme expression (Fig. 11C) may be a transcriptional

LFD-fed (C) and HFD-fed (D) mice. E: Ambulatory activity total over 24-h. F: Energy expenditure AUC over 24-h. G: RER values over 24 h period. H: Twenty-four hour average of RER values. Time graph data were binned into 2 h averages with light/dark cycle shown. Data are expressed as average  $\pm$  SEM (n = 6). \**P* < 0.05 compared with control group of the same diet.

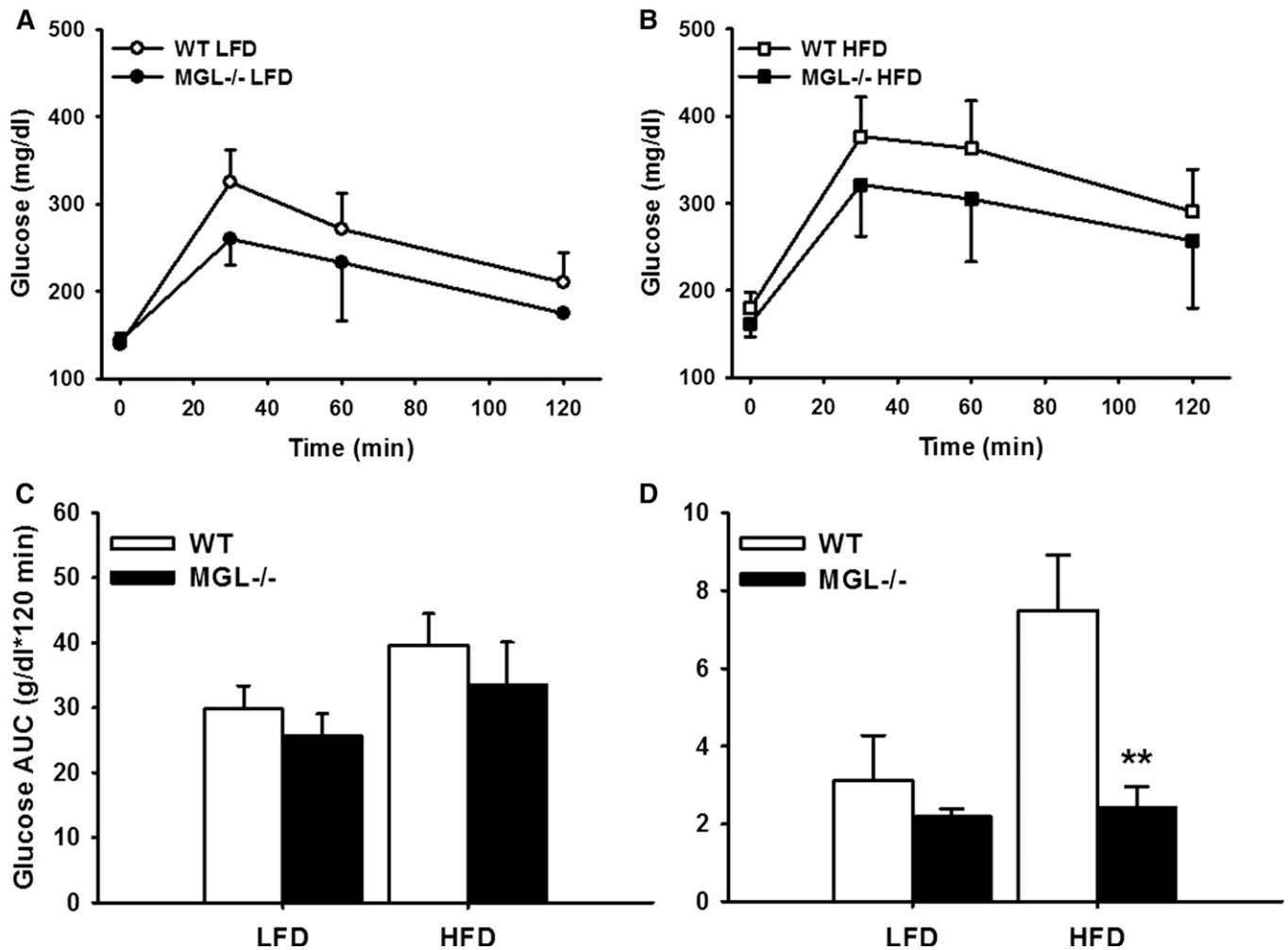


**Fig. 9.** OGTT of male mice at endpoint (11 weeks of diet feeding). LFD-fed mice OGTT (A), HFD-fed mice OGTT (B), and AUC for OGTT (C). D: HOMA-IR values using fasted blood glucose and insulin. Data are expressed as average  $\pm$  SEM ( $n = 6$ ). \*\* $P < 0.01$  compared with control group of the same diet.

response to an overabundance of MG in the postprandial state and therefore compensate for excess MG in the MGL<sup>-/-</sup> mice by increasing its incorporation into TG. This is further supported by a concomitant decrease in GPAT expression (Fig. 11C), which becomes less necessary to generate glycerolipid precursors when MG is already present for TG synthesis. Indeed, previous studies have demonstrated the inhibition of the glycerol-3-phosphate pathway in intestinal mucosa by the addition of excess 2-MG (57). By contrast, in other tissues such as liver, where most TG synthesis occurs through the glycerol-3-phosphate pathway (58), MGL deletion had no apparent effect on the expression of GPAT, and intracellular MG levels were many fold higher than those in the WT mice.

The striking reduction in the appearance of blood TG following oral fat challenge indicates that MGL deficiency has a dramatic effect on intestinal lipid processing and/or secretion. For this particular experiment in which a large bolus of fat is administered orally, we attribute most of this alteration in circulating TG to be due to intestinal changes. However, this does not entirely preclude the contribution of the liver to systemic TG levels.

While we and others did not observe any changes in hepatic lipogenic gene expression that would be indicative of reduced TG synthesis and VLDL production, reductions in adipose lipolysis and VLDL production have been noted in a previous study of MGL-null mice (35). This suggests that smaller visceral fat depots and a smaller circulating FFA pool may limit hepatic reesterification and secretion of TG, which may also contribute to the lower plasma lipids we observed in fasted mice. Interestingly, the oral fat challenge results are similar to those in MGAT2- and DGAT1-deficient mice, that, despite having quantitatively normal intestinal fat absorption overall, also have largely reduced TG appearance rates in OFTTs (6, 59). Both knockout strains are also resistant to diet-induced obesity and have increased energy expenditure through up-regulation of FA oxidation (6, 7, 60). Given that intestine-specific expression of MGAT2 (61) or DGAT1 (62) partially or completely abolishes the lean phenotype in their respective global knockouts, it is possible that intestinal TG metabolism and secretion is a critical determinant of fat utilization and body composition. This in turn may underlie the phenotype we observed in the MGL<sup>-/-</sup> mice.

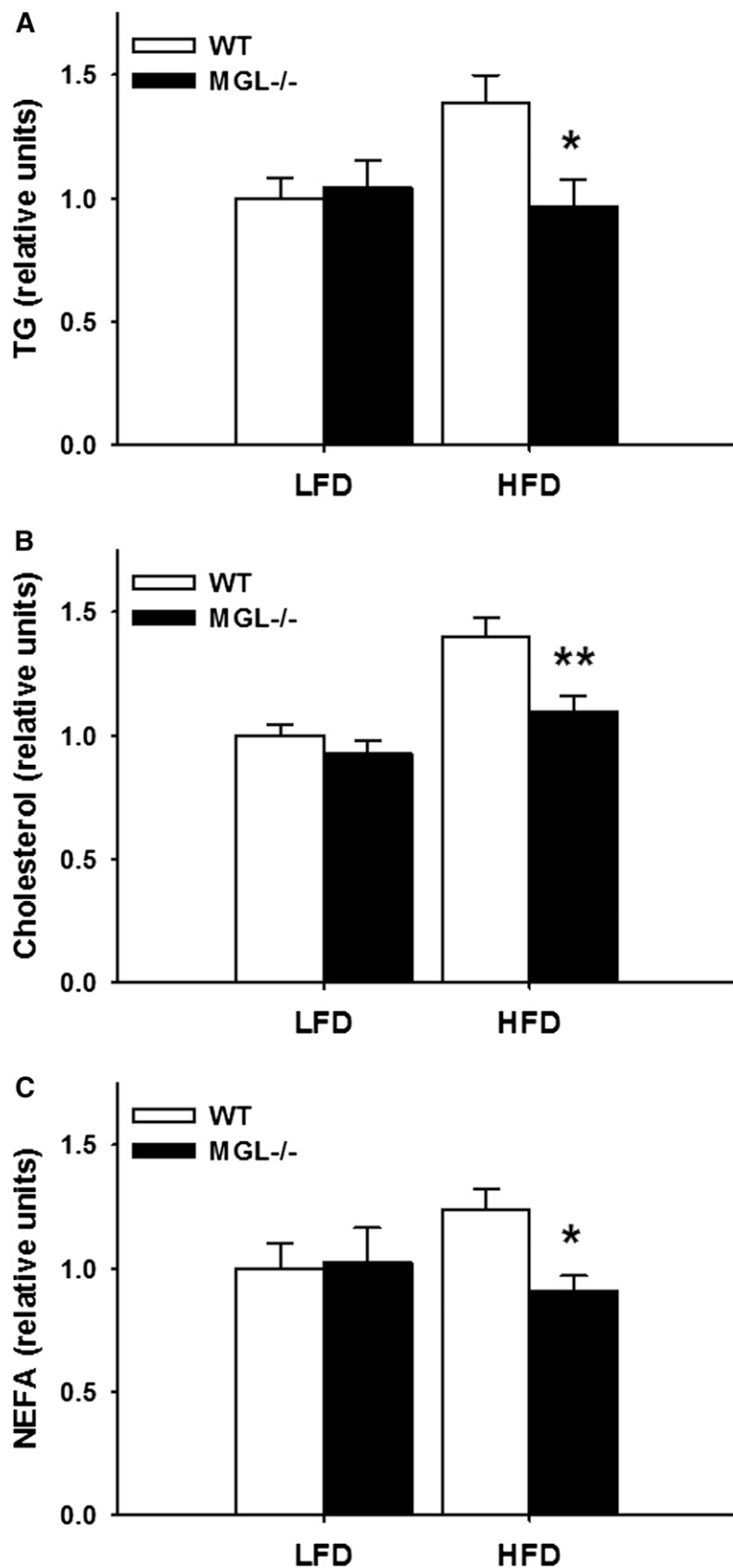


**Fig. 10.** Plasma lipids in 12 h fasted mice after 12 weeks of LFD or HFD feeding. TG (A); Total cholesterol (B), and NEFA (C). Data from each male and female group were normalized to WT LFD and then both sexes combined. Data are expressed as average  $\pm$  SEM (n = 11–12). \* $P$  < 0.05, \*\* $P$  < 0.01 compared with control group of the same diet.

Still, it is unknown whether the delayed entry of fat into the circulation of MGL<sup>-/-</sup> and MGAT2<sup>-/-</sup> mice proceeds through similar mechanisms. However, these two mouse lines share a common inability to process MG normally in

the small intestine and other tissues. This raises the possibility that the pathways are indeed similar and further underscores the importance of intestinal MG metabolism in dietary lipid assimilation.

TABLE 3. Plasma peptide levels in male mice as analyzed by multiplex immunoassay

Analyte (pg/ml)	WT LFD	MGL <sup>-/-</sup> LFD	WT HFD	MGL <sup>-/-</sup> HFD
Insulin	333 ± 103	249 ± 21	724 ± 196	255 ± 56 <sup>a</sup>
Glucagon	47 ± 5	69 ± 8 <sup>a</sup>	45 ± 9	43 ± 9
C-peptide	634 ± 166	298 ± 55	883 ± 164	382 ± 85 <sup>a</sup>
PP	18 ± 3	38 ± 10	17 ± 4	23 ± 6
Leptin (ng/ml)	12 ± 2	4 ± 2 <sup>a</sup>	27 ± 4	18 ± 3
Adiponectin (ng/ml)	15 ± 1	14 ± 1	13 ± 1	15 ± 1
Resistin (ng/ml)	14 ± 2	10 ± 1 <sup>a</sup>	25 ± 3	14 ± 2 <sup>a</sup>
GIP	161 ± 28	126 ± 40	145 ± 46	102 ± 16
PYY	105 ± 8	103 ± 9	112 ± 22	79 ± 13
MCP-1	87 ± 20	44 ± 12	103 ± 14	89 ± 22
TNFα	23 ± 7	19 ± 2	20 ± 5	32 ± 3
IL-6	48 ± 15	44 ± 15	85 ± 61	52 ± 20

Data are expressed as average ± SEM (n = 5–6).

<sup>a</sup>P < 0.05 compared with control group of the same diet.

Although, as noted, relatively little has been reported about the effects of MGL gene deletion on body weight gain and associated metabolic processes, the results to date are somewhat conflicting. In a study by Chanda et al. (19), both male and female adult MGL<sup>-/-</sup> mice showed a 16.5% reduction in body weight, which persisted over time. This decreased body weight is similar to those seen in CBI<sup>-/-</sup> mice and in CBI antagonist-treated mice (22). In contrast, Taschler et al. (35) did not observe changes in the weight or body composition of MGL<sup>-/-</sup> mice fed either an 11% (kilocalories) chow diet or a 74% (kilocalories) very HFD for 12 weeks. Underlying reasons for this discrepancy between phenotype in the studies remain unclear. Both used gene targeting methods to generate the knockout mice, albeit with different targeting vectors, and both mouse lines have similar genetic backgrounds, C57Bl6 (35) and C57Bl6/NTac (19). Differences in diet composition, and particularly fat sources, between the studies could potentially contribute to phenotypic differences; however, this information was not available. In the present study, controlled semipurified diets of defined composition were used, which differed in the percent of energy as fat. Moreover, the HFD was set at 45% of total calories to more closely reflect physiological levels of fat intake. The reduced body mass gain that was found here in both male and female MGL<sup>-/-</sup> mice was consistent with results from Chanda et al. (19). It is worth noting that the degree of reduction in body mass was not as pronounced on the 45% fat diet as it was on the 10% fat diet. Together with the absence of an effect in Taschler et al. (35), at least on the 74% fat diet, this could reflect desensitization of CB1 receptors by continuous marked elevations of 2-AG levels.

A detailed week-long analysis of LFD feeding behavior, performed immediately after the 12 weeks of LFD intake, revealed an apparent dysregulation in circadian food intake. The MGL-null mice ate relatively more during the light phase than WT mice, which contributed to an overall larger caloric intake. Alterations in food intake had not been found during the initial 12 weeks on the diet, however the crude pellet weight method would not likely be sensitive enough to discern small differences. A potential mechanism for the increased light phase feeding may be the natural diurnal variations in brain CB1 receptor expression (63) and 2-AG and AEA levels (64). Certainly,

central EC signaling is an important regulator of eating behaviors (21–24). Thus, any loss of EC function as a result of MGL deletion may disrupt normal patterns of eating behavior. It will be necessary in future studies to use time-dependent inhibition of MGL to better understand this effect on circadian food intake pattern. Acute administration of the MGL inhibitor JZL184 or 2-AG both stimulate short-term feeding behavior (38, 65), however, the effects of chronic MGL inhibition, and its associated 2-AG elevation, on food intake and energy balance have not been reported. Intermittent elevation of 2-AG may be a potential method for avoiding EC desensitization. Interestingly, it has been shown that CB1-mediated analgesia is sustained by repeated low-dose administration of the irreversible MGL inhibitor, JZL184 (66). Additionally, use of other MGL inhibitors with different kinetics, such as reversible inhibitors that dissociate quickly, may also avoid the desensitization of the EC system and provide a clearer picture of the temporal effects of short-term MGL inactivation.

Taschler et al. (35) found that MGL deletion in mice mitigated HFD-induced insulin resistance. Whether this points to a pathogenic role of MGL in the liberation of FFA associated with inflammation and obesity-related illnesses remains to be seen. Certainly, the decreased levels of resistin shown in the present study provide further evidence that MGL deletion confers some protection against the development of insulin resistance. In the murine model, resistin is an adipocyte-derived cytokine that has been suggested to be an important link between obesity and type 2 diabetes mellitus (67). Increasing the levels of circulating resistin in mice through transgenic overexpression (68) or recombinant treatment (69) causes insulin resistance, whereas genetic deletion preserves insulin sensitivity in obese mice (70). Additionally, given the broad acyl chain substrate specificity of MGL (15), the possibility that elevations of MG species other than 2-AG may be aiding in glucose disposal through newly discovered pathways cannot be ruled out. Notably, 2-oleoylglycerol has recently been shown to bind GPR119 receptors in enteroendocrine and pancreatic β-cells, stimulating the release of glucagon-like peptide 1 and insulin, respectively (71, 72).


A potentially beneficial consequence of MGL inhibition or gene deletion is the sequestering of arachidonic acid (AA) in the form of 2-AG. Brain AA levels were found to be

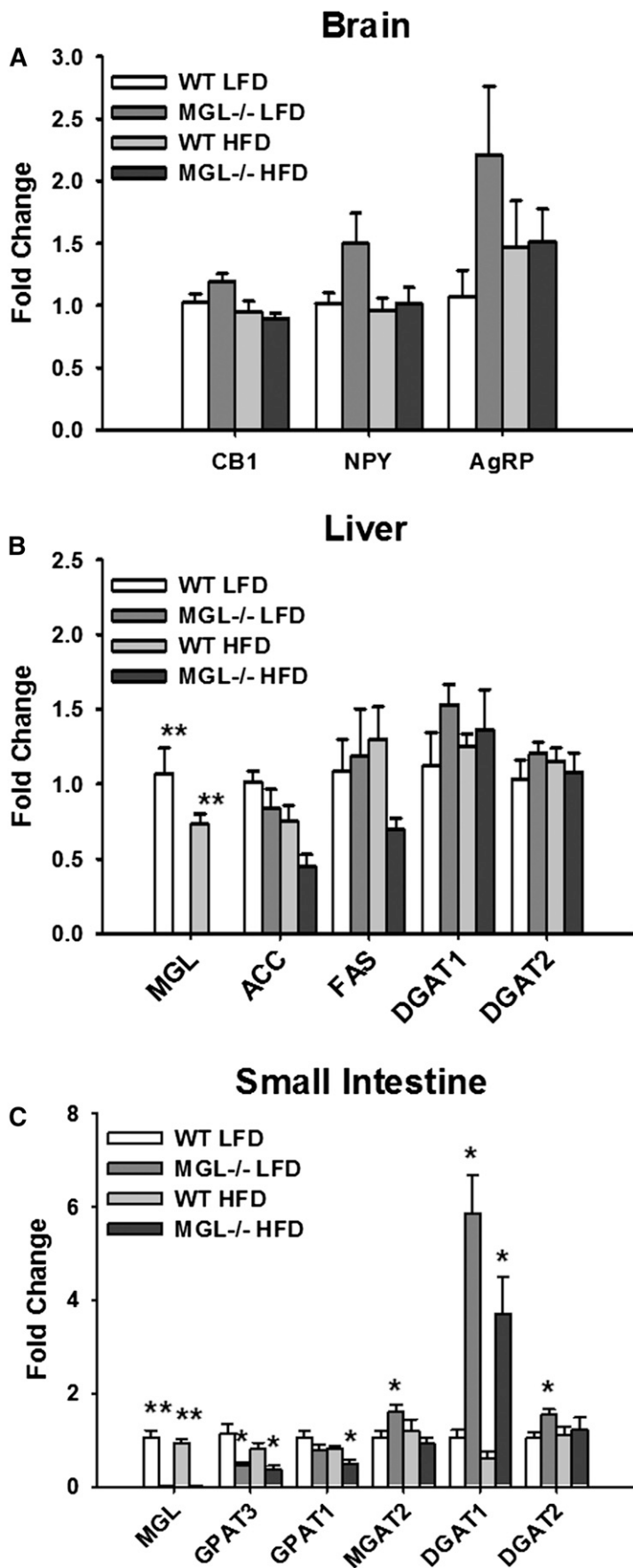


**Fig. 11.** Tissue gene expression measured by RT-PCR and analyzed by the ddCT method in brain (A), liver (B), and small intestine mucosa (C). All transcript levels are presented relative to the WT LFD group. Data are expressed as average  $\pm$  SEM (n = 5–6). \* $P$  < 0.05, \*\* $P$  < 0.001 compared with control group of the same diet.



significantly reduced alongside elevations in 2-AG in MGL<sup>-/-</sup> mice (32), similar to those found in the present study. Because the majority of AA used in prostaglandin production is thought to be derived from 2-AG catabolism (48), beneficial effects on diseases from cancer to hepatic ischemia have been ascribed to MGL knockout or pharmacological inhibition (73–75). In fact, MGL inhibition appears to limit progression of neurodegenerative disorders, such as Parkinson's and Alzheimer's disease, both by decreasing prostaglandin production and by the anti-inflammatory effect of CB2 stimulation by 2-AG (48, 76). Considering the interrelationships between inflammation and metabolic function (77), it is therefore possible that alterations in these signaling pathways underlie the healthier phenotype observed here in the MGL<sup>-/-</sup> mice, including trends for reductions in cytokines such as MCP-1.

In summary, the present studies show that genetic deletion of MGL in mice results in high tissue levels of MG. For the intestine, there was evidence of upregulation of the already predominant pathway of intestinal TG synthesis via MGAT and DGAT. MGL<sup>-/-</sup> mice on both LFD and HFD had reduced weight gain over the 12 weeks of feeding, and when dietary fat was limited, MGL<sup>-/-</sup> mice were significantly leaner and displayed increased fat oxidation. Serum lipid levels were decreased, as were many signaling peptides involved in maintaining energy homeostasis. MGL<sup>-/-</sup> mice also had a greatly reduced rate of intestinal TG secretion. These results suggest that large reductions in MGL hydrolysis have the potential to affect whole body energy homeostasis, as well as to be protective against some of the deleterious downstream effects of HFD-induced obesity. 

The authors thank Sandy Wilson at Janssen Research & Development, LLC for technical assistance. Use of the BioDAQ instrument was made possible by Research Diets, Inc., with assistance from Doug Compton.

## REFERENCES

- Phan, C. T., and P. Tso. 2001. Intestinal lipid absorption and transport. *Front. Biosci.* **6**: D299–D319.
- Labar, G., J. Wouters, and D. M. Lambert. 2010. A review on the monoacylglycerol lipase: at the interface between fat and endocannabinoid signalling. *Curr. Med. Chem.* **17**: 2588–2607.
- Stella, N., P. Schweitzer, and D. Piomelli. 1997. A second endogenous cannabinoid that modulates long-term potentiation. *Nature.* **388**: 773–778.
- Fonseca, B. M., M. A. Costa, M. Almada, G. Correia-da-Silva, and N. A. Teixeira. 2013. Endogenous cannabinoids revisited: A biochemistry perspective. *Prostaglandins Other Lipid Mediat.* **102–103**: 13–30.
- Gao, Y., D. V. Vasilyev, M. B. Goncalves, F. V. Howell, C. Hobbs, M. Reisenberg, R. Shen, M-Y. Zhang, B. W. Strassle, P. Lu, et al. 2010. Loss of retrograde endocannabinoid signaling and reduced adult neurogenesis in diacylglycerol lipase knock-out mice. *J. Neurosci.* **30**: 2017–2024.
- Yen, C-L. E., M-L. Cheong, C. Grueter, P. Zhou, J. Moriwaki, J. S. Wong, B. Hubbard, S. Marmor, and R. V. Farese. 2009. Deficiency of the intestinal enzyme acyl CoA:monoacylglycerol acyltransferase-2 protects mice from metabolic disorders induced by high-fat feeding. *Nat. Med.* **15**: 442–446.
- Smith, S. J., S. Cases, D. R. Jensen, H. C. Chen, E. Sande, B. Tow, D. A. Sanan, J. Raber, R. H. Eckel, and R. V. Farese. 2000. Obesity resistance and multiple mechanisms of triglyceride synthesis in mice lacking Dgat. *Nat. Genet.* **25**: 87–90.
- Long, J. Z., W. Li, L. Booker, J. J. Burston, S. G. Kinsey, J. E. Schlosburg, F. J. Pavón, A. M. Serrano, D. E. Selley, L. H. Parsons, et al. 2009. Selective blockade of 2-arachidonoylglycerol hydrolysis produces cannabinoid behavioral effects. *Nat. Chem. Biol.* **5**: 37–44.
- Blankman, J. L., G. M. Simon, and B. F. Cravatt. 2007. A comprehensive profile of brain enzymes that hydrolyze the endocannabinoid 2-arachidonoylglycerol. *Chem. Biol.* **14**: 1347–1356.
- Tornqvist, H., and P. Beltrage. 1976. Purification and some properties of a monoacylglycerol-hydrolyzing enzyme of rat adipose tissue. *J. Biol. Chem.* **251**: 813–819.
- Karlsson, M., J. A. Contreras, U. Hellman, H. Tornqvist, and C. Holm. 1997. cDNA cloning, tissue distribution, and identification of the catalytic triad of monoglyceride lipase. Evolutionary relationship to esterases, lysophospholipases, and haloperoxidases. *J. Biol. Chem.* **272**: 27218–27223.
- Karlsson, M., K. Reue, Y. R. Xia, A. J. Lusis, D. Langin, H. Tornqvist, and C. Holm. 2001. Exon-intron organization and chromosomal localization of the mouse monoglyceride lipase gene. *Gene.* **272**: 11–18.
- Chon, S-H., J. D. Douglass, Y. X. Zhou, N. Malik, J. L. Dixon, A. Brinker, L. Quadro, and J. Storch. 2012. Over-expression of monoacylglycerol lipase (MGL) in small intestine alters endocannabinoid levels and whole body energy balance, resulting in obesity. *PLoS ONE.* **7**: e43962.
- Rindlisbacher, B., M. Reist, and P. Zahler. 1987. Diacylglycerol breakdown in plasma membranes of bovine chromaffin cells is a two-step mechanism mediated by a diacylglycerol lipase and a monoacylglycerol lipase. *Biochim. Biophys. Acta.* **905**: 349–357.
- Vandevoorde, S., B. Saha, A. Mahadevan, R. K. Razdan, R. G. Pertwee, B. R. Martin, and C. J. Fowler. 2005. Influence of the degree of unsaturation of the acyl side chain upon the interaction of analogues of 1-arachidonoylglycerol with monoacylglycerol lipase and fatty acid amide hydrolase. *Biochem. Biophys. Res. Commun.* **337**: 104–109.
- Ghafouri, N., G. Tiger, R. K. Razdan, A. Mahadevan, R. G. Pertwee, B. R. Martin, and C. J. Fowler. 2004. Inhibition of monoacylglycerol lipase and fatty acid amide hydrolase by analogues of 2-arachidonoylglycerol. *Br. J. Pharmacol.* **143**: 774–784.
- Dinh, T. P., S. Kathuria, and D. Piomelli. 2004. RNA interference suggests a primary role for monoacylglycerol lipase in the degradation of the endocannabinoid 2-arachidonoylglycerol. *Mol. Pharmacol.* **66**: 1260–1264.
- Saario, S. M., O. M. H. Salo, T. Nevalainen, A. Poso, J. T. Laitinen, T. Järvinen, and R. Niemi. 2005. Characterization of the sulfhydryl-sensitive site in the enzyme responsible for hydrolysis of 2-arachidonoylglycerol in rat cerebellar membranes. *Chem. Biol.* **12**: 649–656.
- Chanda, P. K., Y. Gao, L. Mark, J. Btsh, B. W. Strassle, P. Lu, M. J. Piesla, M-Y. Zhang, B. Bingham, A. Uveges, et al. 2010. Monoacylglycerol lipase activity is a critical modulator of the tone and integrity of the endocannabinoid system. *Mol. Pharmacol.* **78**: 996–1003.
- Di Marzo, V. 2009. The endocannabinoid system: its general strategy of action, tools for its pharmacological manipulation and potential therapeutic exploitation. *Pharmacol. Res.* **60**: 77–84.
- Di Marzo, V., and I. Matias. 2005. Endocannabinoid control of food intake and energy balance. *Nat. Neurosci.* **8**: 585–589.
- Di Marzo, V., S. K. Goparaju, L. Wang, J. Liu, S. Bátkai, Z. Járjai, F. Fezza, G. I. Miura, R. D. Palmiter, T. Sugiura, et al. 2001. Leptin-regulated endocannabinoids are involved in maintaining food intake. *Nature.* **410**: 822–825.
- Cota, D., G. Marsicano, B. Lutz, V. Vicennati, G. K. Stalla, R. Pasquali, and U. Pagotto. 2003. Endogenous cannabinoid system as a modulator of food intake. *Int. J. Obes. Relat. Metab. Disord.* **27**: 289–301.
- Horvath, T. L. 2003. Endocannabinoids and the regulation of body fat: the smoke is clearing. *J. Clin. Invest.* **112**: 323–326.
- Cota, D., G. Marsicano, M. Tschöp, Y. Grübler, C. Flachskamm, M. Schubert, D. Auer, A. Yassouridis, C. Thöne-Reineke, S. Ortmann, et al. 2003. The endogenous cannabinoid system affects energy balance via central orexigenic drive and peripheral lipogenesis. *J. Clin. Invest.* **112**: 423–431.
- Kunos, G., and D. Osei-Hyiaman. 2008. Endocannabinoids and liver disease. IV. Endocannabinoid involvement in obesity and

- hepatic steatosis. *Am. J. Physiol. Gastrointest. Liver Physiol.* **294**: G1101–G1104.
27. Osei-Hyiaman, D., M. DePetrillo, P. Pacher, J. Liu, S. Radaeva, S. Bátkai, J. Harvey-White, K. Mackie, L. Offertaler, L. Wang, et al. 2005. Endocannabinoid activation at hepatic CB1 receptors stimulates fatty acid synthesis and contributes to diet-induced obesity. *J. Clin. Invest.* **115**: 1298–1305.
  28. Kunos, G., D. Osei-Hyiaman, J. Liu, G. Godlewski, and S. Bátkai. 2008. Endocannabinoids and the control of energy homeostasis. *J. Biol. Chem.* **283**: 33021–33025.
  29. Burdyga, G., A. Varro, R. Dimaline, D. G. Thompson, and G. J. Dockray. 2010. Expression of cannabinoid CB1 receptors by vagal afferent neurons: kinetics and role in influencing neurochemical phenotype. *Am. J. Physiol. Gastrointest. Liver Physiol.* **299**: G63–G69.
  30. Gómez, R., M. Navarro, M. Trigo, A. Bilbao, I. Del Arco, A. Cippitelli, F. Nava, D. Piomelli, and F. Rodríguez. 2002. A peripheral mechanism for CB1 cannabinoid receptor-dependent modulation of feeding. *J. Neurosci.* **22**: 9612–9617.
  31. Kinsey, S. G., J. Z. Long, S. T. O'Neal, R. A. Abdullah, J. L. Poklis, D. L. Boger, B. F. Cravatt, and A. H. Lichtman. 2009. Blockade of endocannabinoid-degrading enzymes attenuates neuropathic pain. *J. Pharmacol. Exp. Ther.* **330**: 902–910.
  32. Schlosburg, J. E., J. L. Blankman, J. Z. Long, D. K. Nomura, B. Pan, S. G. Kinsey, P. T. Nguyen, D. Ramesh, L. Booker, J. J. Burston, et al. 2010. Chronic monoacylglycerol lipase blockade causes functional antagonism of the endocannabinoid system. *Nat. Neurosci.* **13**: 1113–1119.
  33. Zhong, P., B. Pan, X. Gao, J. L. Blankman, B. F. Cravatt, and Q. Liu. 2011. Genetic deletion of monoacylglycerol lipase alters endocannabinoid-mediated retrograde synaptic depression in the cerebellum. *J. Physiol.* **589**: 4847–4855.
  34. Pan, B., W. Wang, P. Zhong, J. L. Blankman, B. F. Cravatt, and Q. S. Liu. 2011. Alterations of endocannabinoid signaling, synaptic plasticity, learning, and memory in monoacylglycerol lipase knock-out mice. *J. Neurosci.* **31**: 13420–13430.
  35. Taschler, U., F. P. W. Radner, C. Heier, R. Schreiber, M. Schweiger, G. Schoiswohl, K. Preiss-Landl, D. Jaeger, B. Reiter, H. C. Koefeler, et al. 2011. Monoglyceride lipase-deficiency in mice impairs lipolysis and attenuates diet-induced insulin resistance. *J. Biol. Chem.* **286**: 17467–17477.
  36. Ho, S-Y., L. Delgado, and J. Storch. 2002. Monoacylglycerol metabolism in human intestinal Caco-2 cells: evidence for metabolic compartmentation and hydrolysis. *J. Biol. Chem.* **277**: 1816–1823.
  37. Chon, S-H., Y. X. Zhou, J. L. Dixon, and J. Storch. 2007. Intestinal monoacylglycerol metabolism: developmental and nutritional regulation of monoacylglycerol lipase and monoacylglycerol acyltransferase. *J. Biol. Chem.* **282**: 33346–33357.
  38. Kirkham, T. C., C. M. Williams, F. Fezza, and V. Di Marzo. 2002. Endocannabinoid levels in rat limbic forebrain and hypothalamus in relation to fasting, feeding and satiation: stimulation of eating by 2-arachidonoyl glycerol. *Br. J. Pharmacol.* **136**: 550–557.
  39. Zambrowicz, B. P., and G. A. Friedrich. 1998. Comprehensive mammalian genetics: history and future prospects of gene trapping in the mouse. *Int. J. Dev. Biol.* **42**: 1025–1036.
  40. McLean, J. A., and G. Tobin. 1987. Animal and Human Calorimetry. Cambridge University Press, Cambridge, UK.
  41. Bradford, M. M. 1976. A rapid and sensitive method for the quantitation of microgram quantities of protein utilizing the principle of protein-dye binding. *Anal. Biochem.* **72**: 248–254.
  42. Storch, J., Y. X. Zhou, and W. S. Lagakos. 2008. Metabolism of apical versus basolateral sn-2-monoacylglycerol and fatty acids in rodent small intestine. *J. Lipid Res.* **49**: 1762–1769.
  43. Folch, J., M. Less, and S. Stone. 1957. A simple method for the isolation and purification of total lipids from animal tissues. *J. Biol. Chem.* **226**: 497–509.
  44. Dill, M. J., J. Shaw, J. Cramer, and D. K. Sindelar. 2013. 5-HT1A receptor antagonists reduce food intake and body weight by reducing total meals with no conditioned taste aversion. *Pharmacol. Biochem. Behav.* **112**: 1–8.
  45. Chomczynski, P., and N. Sacchi. 1987. Single-step method of RNA isolation by acid guanidinium thiocyanate-phenol-chloroform extraction. *Anal. Biochem.* **162**: 156–159.
  46. Douglass, J. D., N. Malik, S-H. Chon, K. Wells, Y. X. Zhou, A. S. Choi, L. B. Joseph, and J. Storch. 2012. Intestinal mucosal triacylglycerol accumulation secondary to decreased lipid secretion in obese and high fat fed mice. *Front. Physiol.* **3**: 25.
  47. Matthews, D. R., J. P. Hosker, A. S. Rudenski, B. A. Naylor, D. F. Treacher, and R. C. Turner. 1985. Homeostasis model assessment: insulin resistance and beta-cell function from fasting plasma glucose and insulin concentrations in man. *Diabetologia.* **28**: 412–419.
  48. Nomura, D. K., B. E. Morrison, J. L. Blankman, J. Z. Long, S. G. Kinsey, M. C. G. Marcondes, A. M. Ward, Y. K. Hahn, A. H. Lichtman, B. Conti, et al. 2011. Endocannabinoid hydrolysis generates brain prostaglandins that promote neuroinflammation. *Science.* **334**: 809–813.
  49. Hildebrandt, A. L., D. M. Kelly-Sullivan, and S. C. Black. 2003. Antiobesity effects of chronic cannabinoid CB1 receptor antagonist treatment in diet-induced obese mice. *Eur. J. Pharmacol.* **462**: 125–132.
  50. Ravinet Trillou, C., C. Delgorge, C. Menet, M. Arnone, and P. Soubrié. 2004. CB1 cannabinoid receptor knockout in mice leads to leanness, resistance to diet-induced obesity and enhanced leptin sensitivity. *Int. J. Obes. Relat. Metab. Disord.* **28**: 640–648.
  51. Johnston, J. M., G. A. Rao, and P. A. Lowe. 1967. The separation of the alpha-glycerophosphate and monoglyceride pathways in the intestinal biosynthesis of triglycerides. *Biochim. Biophys. Acta.* **137**: 578–580.
  52. Eckel, R. H., S. M. Grundy, and P. Z. Zimmet. 2010. The metabolic syndrome. *Lancet.* **375**: 181–183.
  53. Zhang, L-N., Y. Gamo, R. Sinclair, S. E. Mitchell, D. G. Morgan, J. C. Clapham, and J. R. Speakman. 2012. Effects of chronic oral rimonabant administration on energy budgets of diet-induced obese C57BL/6 mice. *Obesity (Silver Spring).* **20**: 954–962.
  54. Di Marzo, V. 2008. The endocannabinoid system in obesity and type 2 diabetes. *Diabetologia.* **51**: 1356–1367.
  55. Kozak, K. R., B. C. Crews, J. D. Morrow, L-H. Wang, Y. H. Ma, R. Weinander, P.J. Jakobsson, and L. J. Marnett. 2002. Metabolism of the endocannabinoids, 2-arachidonoylglycerol and anandamide, into prostaglandin, thromboxane, and prostacyclin glycerol esters and ethanolamides. *J. Biol. Chem.* **277**: 44877–44885.
  56. Silvestri, C., and V. Di Marzo. 2013. The endocannabinoid system in energy homeostasis and the etiopathology of metabolic disorders. *Cell Metab.* **17**: 475–490.
  57. Polheim, D., J. S. David, F. M. Schultz, M. B. Wylie, and J. M. Johnson. 1973. Regulation of triglyceride biosynthesis in adipose and intestinal tissue. *J. Lipid Res.* **14**: 415–421.
  58. Lockwood, J. F., J. Cao, P. Burn, and Y. Shi. 2003. Human intestinal monoacylglycerol acyltransferase: differential features in tissue expression and activity. *Am. J. Physiol. Endocrinol. Metab.* **285**: E927–E937.
  59. Buhman, K. K., S. J. Smith, S. J. Stone, J. J. Repa, J. S. Wong, F. F. Knapp, B. J. Burri, R. L. Hamilton, N. A. Abumrad, and R. V. Farese. 2002. DGAT1 is not essential for intestinal triacylglycerol absorption or chylomicron synthesis. *J. Biol. Chem.* **277**: 25474–25479.
  60. Nelson, D. W., Y. Gao, N. M. Spencer, T. Banh, and C-L. E. Yen. 2011. Deficiency of MGAT2 increases energy expenditure without high-fat feeding and protects genetically obese mice from excessive weight gain. *J. Lipid Res.* **52**: 1723–1732.
  61. Gao, Y., D. W. Nelson, T. Banh, M-I. Yen, and C-L. E. Yen. 2013. Intestine-specific expression of MOGAT2 partially restores metabolic efficiency in Mogat2-deficient mice. *J. Lipid Res.* **54**: 1644–1652.
  62. Lee, B., A. M. Fast, J. Zhu, J-X. Cheng, and K. K. Buhman. 2010. Intestine-specific expression of acyl CoA:diacylglycerol acyltransferase 1 reverses resistance to diet-induced hepatic steatosis and obesity in Dgat1<sup>-/-</sup> mice. *J. Lipid Res.* **51**: 1770–1780.
  63. Martínez-Vargas, M., E. Murillo-Rodríguez, R. González-Rivera, A. Landa, M. Méndez-Díaz, O. Prospéro-García, and L. Navarro. 2003. Sleep modulates cannabinoid receptor 1 expression in the pons of rats. *Neuroscience.* **117**: 197–201.
  64. Valenti, M., D. Viganò, M. G. Casico, T. Rubino, L. Steardo, D. Parolaro, and V. Di Marzo. 2004. Differential diurnal variations of anandamide and 2-arachidonoyl-glycerol levels in rat brain. *Cell. Mol. Life Sci.* **61**: 945–950.
  65. Woodhams, S. G., A. Wong, D. A. Barrett, A. J. Bennett, V. Chapman, and S. P. H. Alexander. 2012. Spinal administration of the monoacylglycerol lipase inhibitor JZL184 produces robust inhibitory effects on nociceptive processing and the development of central sensitization in the rat. *Br. J. Pharmacol.* **167**: 1609–1619.
  66. Kinsey, S. G., L. E. Wise, D. Ramesh, R. Abdullah, D. E. Selley, B. F. Cravatt, and A. H. Lichtman. 2013. Repeated low dose administration of the monoacylglycerol lipase inhibitor JZL184 retains CB1 receptor mediated antinociceptive and gastroprotective effects. *J. Pharmacol. Exp. Ther.* **345**: 492–501.

67. Steppan, C. M., S. T. Bailey, S. Bhat, E. J. Brown, R. R. Banerjee, C. M. Wright, H. R. Patel, R. S. Ahima, and M. A. Lazar. 2001. The hormone resistin links obesity to diabetes. *Nature*. **409**: 307–312.
68. Li, F-P., J. He, Z-Z. Li, Z-F. Luo, L. Yan, and Y. Li. 2009. Effects of resistin expression on glucose metabolism and hepatic insulin resistance. *Endocrine*. **35**: 243–251.
69. Rajala, M. W., S. Obici, P. E. Scherer, and L. Rossetti. 2003. Adipose-derived resistin and gut-derived resistin-like molecule-beta selectively impair insulin action on glucose production. *J. Clin. Invest.* **111**: 225–230.
70. Qi, Y., Z. Nie, Y-S. Lee, N. S. Singhal, P. E. Scherer, M. A. Lazar, and R. S. Ahima. 2006. Loss of resistin improves glucose homeostasis in leptin deficiency. *Diabetes*. **55**: 3083–3090.
71. Lan, H., H. V. Lin, C. F. Wang, M. J. Wright, S. Xu, L. Kang, K. Juhl, J. A. Hedrick, and T. J. Kowalski. 2012. Agonists at GPR119 mediate secretion of GLP-1 from mouse enteroendocrine cells through glucose-independent pathways. *Br. J. Pharmacol.* **165**: 2799–2807.
72. Hansen, K. B., M. M. Rosenkilde, F. K. Knop, N. Wellner, T. A. Diep, J. F. Rehfeld, U. B. Andersen, J. J. Holst, and H. S. Hansen. 2011. 2-Oleoyl glycerol is a GPR119 agonist and signals GLP-1 release in humans. *J. Clin. Endocrinol. Metab.* **96**: E1409–E1417.
73. Nomura, D. K., J. Z. Long, S. Niessen, H. S. Hoover, S-W. Ng, and B. F. Cravatt. 2010. Monoacylglycerol lipase regulates a fatty acid network that promotes cancer pathogenesis. *Cell*. **140**: 49–61.
74. Lombardi, D. P., D. K. Nomura, and B. F. Cravatt. 2010. Blockade of monoacylglycerol lipase impairs prostate cancer cell pathogenicity. *Clin. Transl. Sci.* **3**: S46.
75. Cao, Z., M. M. Mulvihill, P. Mukhopadhyay, H. Xu, K. Erdélyi, E. Hao, E. Holovac, G. Haskó, B. F. Cravatt, D. K. Nomura, et al. 2013. Monoacylglycerol lipase controls endocannabinoid and eicosanoid signaling and hepatic injury in mice. *Gastroenterology*. **144**: 808–817.
76. Chen, R., J. Zhang, Y. Wu, D. Wang, G. Feng, Y-P. Tang, Z. Teng, and C. Chen. 2012. Monoacylglycerol lipase is a therapeutic target for Alzheimer's disease. *Cell Reports*. **2**: 1329–1339.
77. Hotamisligil, G. S. 2006. Inflammation and metabolic disorders. *Nature*. **444**: 860–867.